



# ULTRA-LIGHT BOSON FOR DARK MATTER: MASS AND SELF-INTERACTION

**LUIS A. UREÑA-LÓPEZ**

UNIVERSITY OF GUANAJUATO

IN COLLABORATION WITH:

**TONATIUH MATOS**

**ALMA GONZÁLEZ-MORALES**

**FRANCISCO LINARES**

**ANTONIO HERRERA-MARTIN**

**MARTIN HENDRY**

**JORGE PEÑARRUBIA**

**VICTOR ROBLES**

**DAVID MARSH**

....

# SCALAR FIELDS

# WHAT IS A SCALAR FIELD?

- According to Particle Physics, a scalar field represents a spin-zero boson.
  - The most famous of all is the Higgs boson, one of some which are needed for spontaneous symmetry breaking in the theory. Another example is the QCD axion.
  - Most extensions of the Standard Model of Particle Physics include scalar fields: **axions, moduli, dilaton, ...**
  - Scalar fields are very successful in condensed matter physics, also for symmetry breaking processes.
- It also needs a scalar field **potential**  $V(\phi)$ : the internal energy associated with a given value of the scalar field.

*Higgs potential*

$$\lambda^2(\phi^2 - M^2)^2$$

*Chaotic inflation*

$$(1/2)m^2\phi^2$$

*Axion*

$$\Lambda[1 - \cos(\phi/f_a)]$$

*Quintessence*

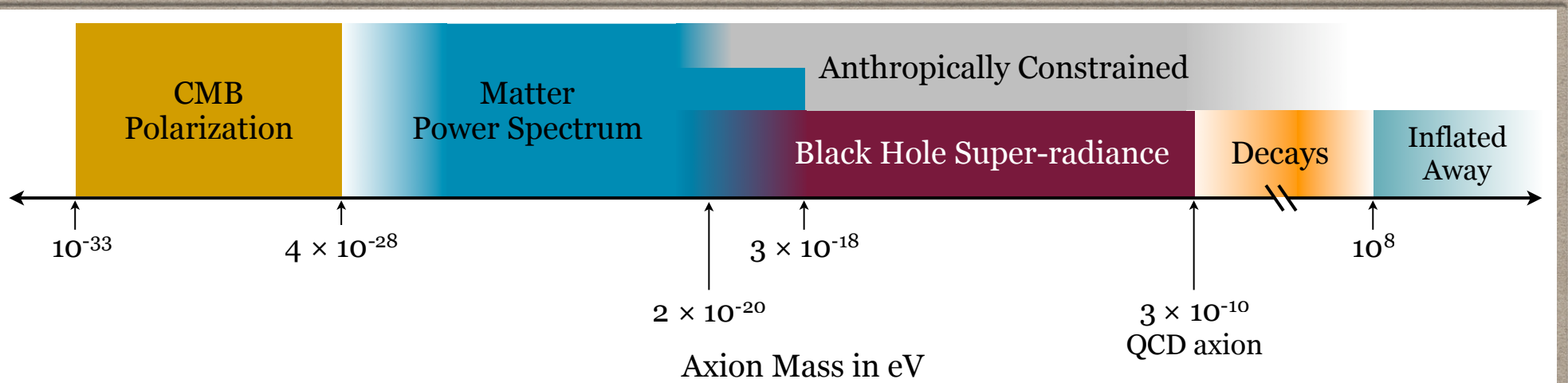
$$V_0 e^{-\lambda\phi/m_{\text{Pl}}}$$

A. Liddle, [http://ned.ipac.caltech.edu/level5/Liddle/Liddle5\\_1.html](http://ned.ipac.caltech.edu/level5/Liddle/Liddle5_1.html)

# **THE AXIVERSE**

String compactifications give rise to many 'axion' fields

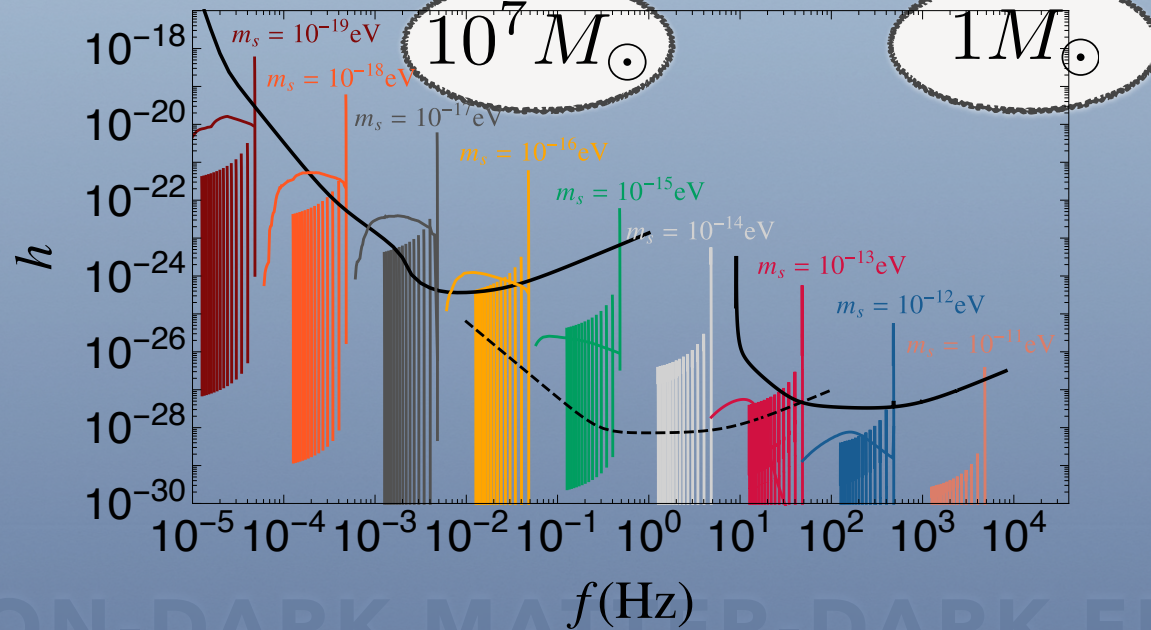
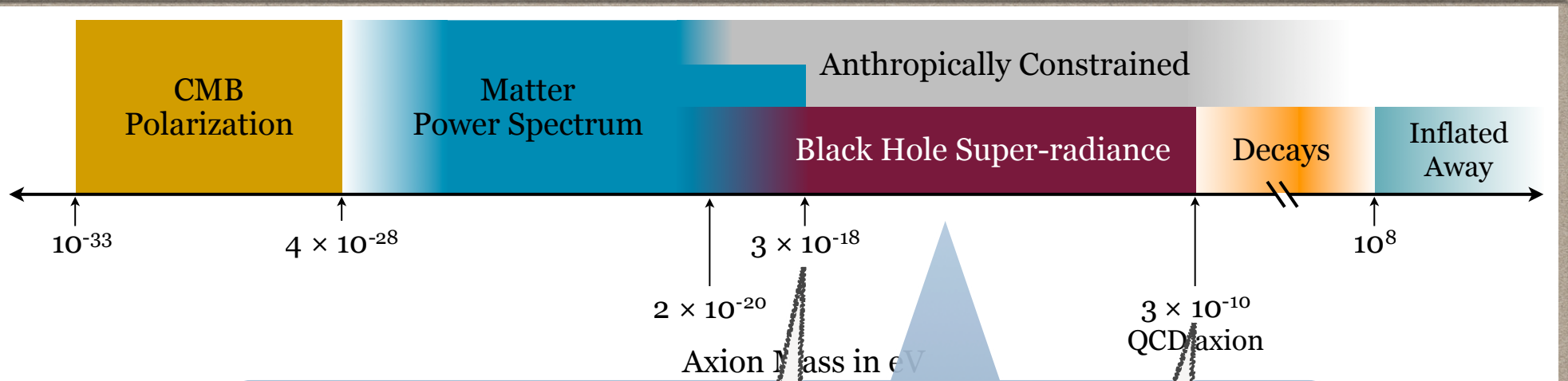
$$V(\phi) = \Lambda_a [1 - \cos(\phi/f_a)] \simeq \begin{cases} 2\Lambda_a & \phi/f_a \sim \pi \\ (\Lambda_a/f_a^2)\phi^2/2 & \phi/f_a \sim 0 \end{cases}$$



Arvanitaki et al, Phys. Rev. D 83, 044026 (2011)

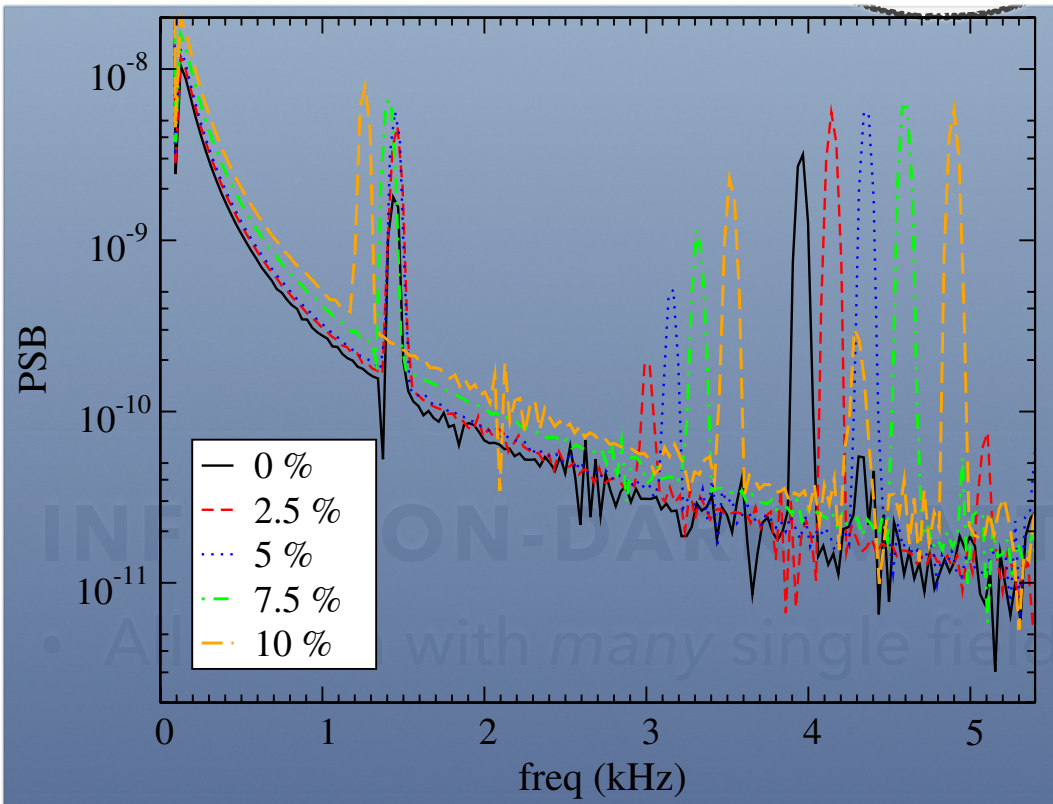
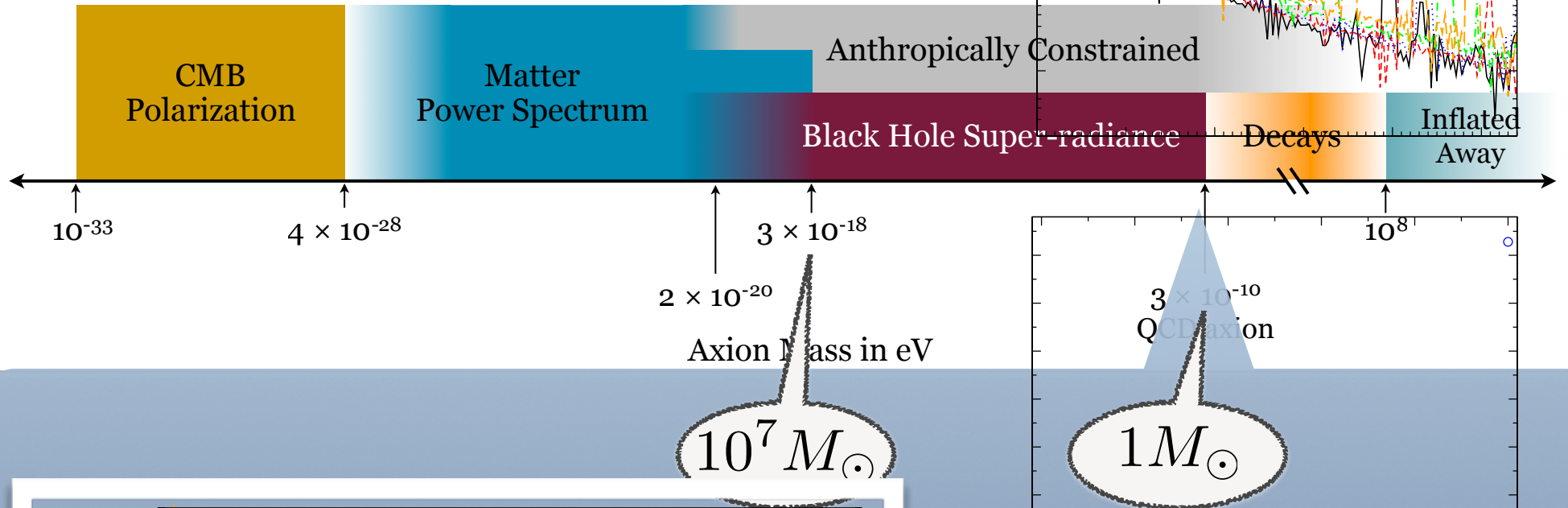
## INFLATION-DARK MATTER-DARK ENERGY

- All in one with *many* single fields: the axiverse



# INFLATION-DARK MATTER-DARK ENERGY

- All action
- FIG. 1. GW strain produced by BH-boson condensates compared to the Advanced LIGO PSD at design sensitivity [47] and to the non-sky averaged LISA PSD [12] (black thick curves), assuming a coherent observation time of  $T_{\text{obs}} = 4$  yr in both cases. Nearly vertical lines

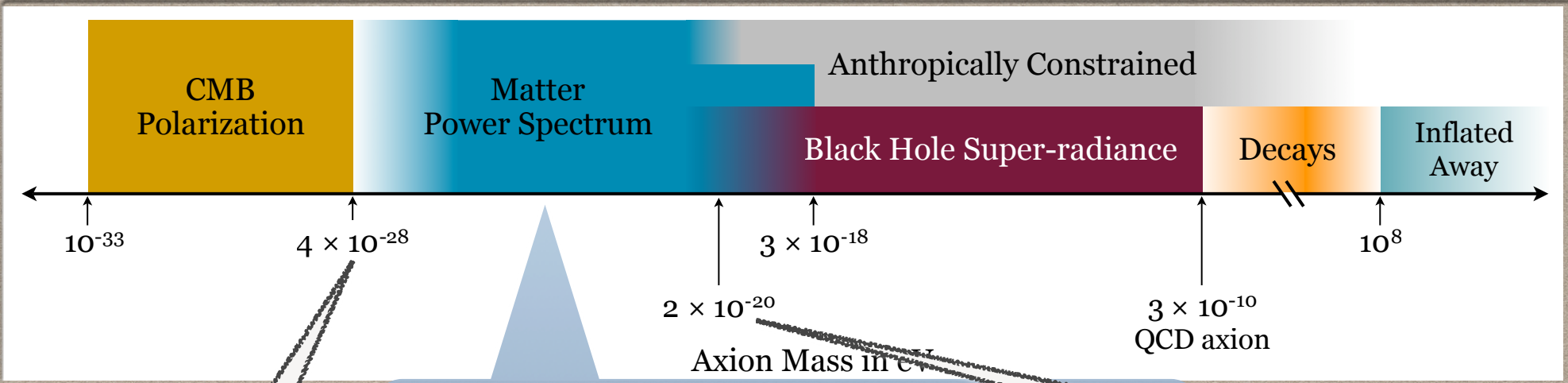


Bosons trapped  
in a neutron star

{0, 2.5, 5, 7.5, 10}% and  $M_T = 1.4$ . (Bottom) Frequencies corresponding to the first, second, and third modes of the isolated neutron star, as a function of the boson fraction. Notice the appearance of new oscillation modes, not present for an isolated neutron star. See the text for more details.

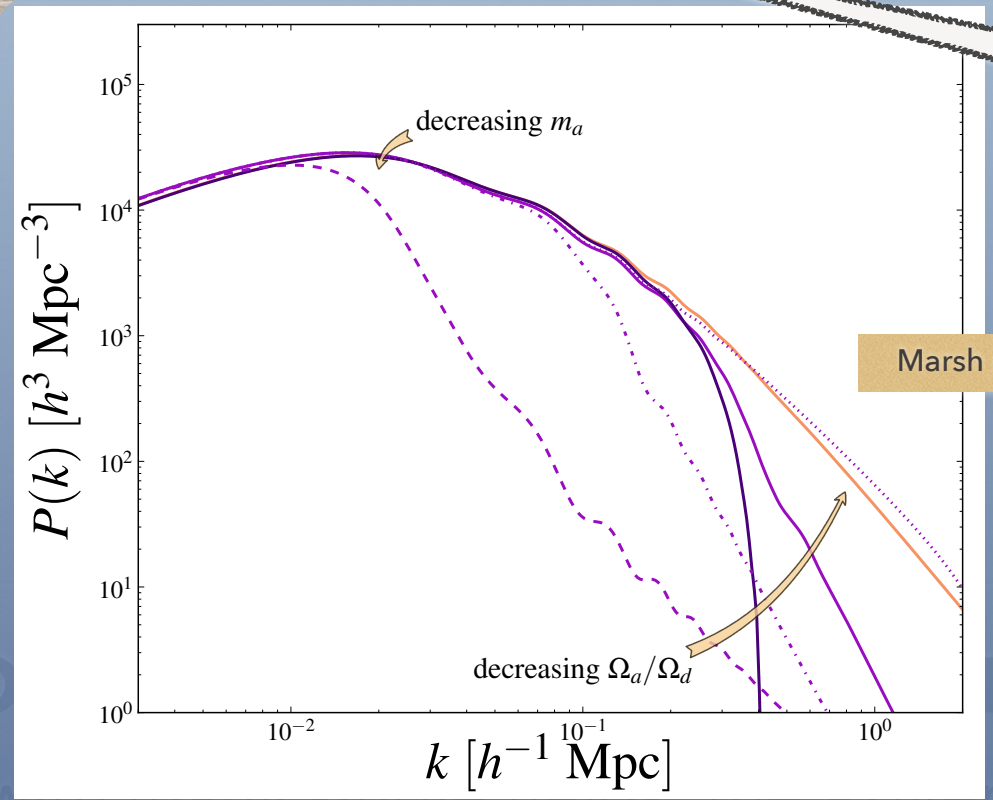
Valdez-Alvarado et al, Phys.Rev. D87 (2013) 8, 084040

Brito et al, Phys.Rev. D93 (2016) no.4, 044045



$10^6 \text{ pc}$

$10^{-2} \text{ pc}$



Marsh et al, Phys. Rev. D 83, 044026 (2011)

INFLATION

• All action with many single fields in the universe

ENERGY

FIG. 1: Adiabatic matter power spectra, with varying axion mass  $m_a = 10^{-28}, 10^{-26}, 10^{-25}, 10^{-23}$  eV at fixed density fraction  $\Omega_a/\Omega_d = 0.5$  (dashed), and varying  $\Omega_a/\Omega_d = 0.1, 0.5, 1$  at fixed  $m_a = 10^{-25}$  eV (solid). Spectra are calculated using the methods of Ref. [23].

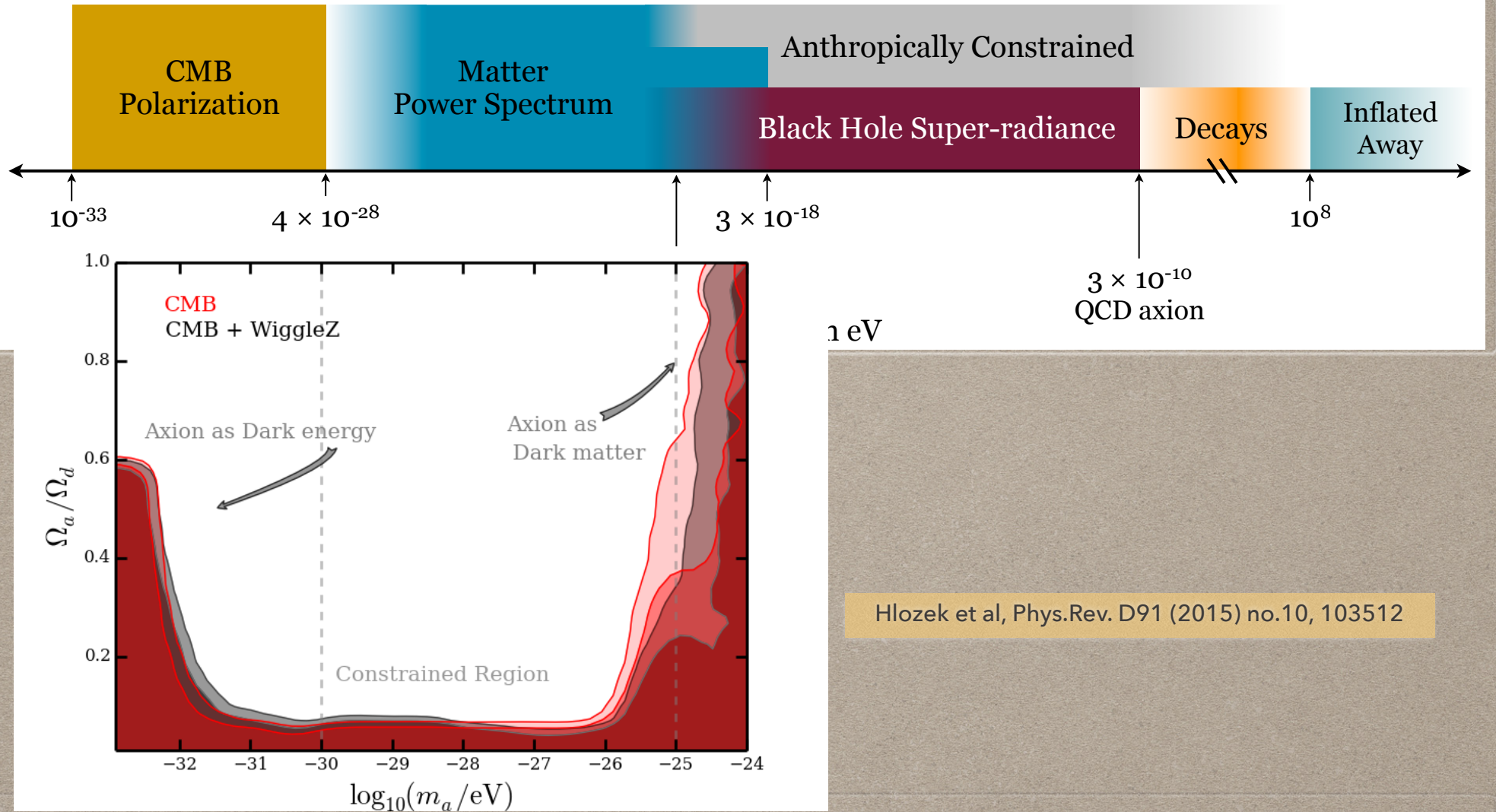


FIG. 1. Marginalized 2 and  $3\sigma$  contours show limits to the ultra-light axion (ULA) mass fraction  $\Omega_a/\Omega_d$  as a function of ULA mass  $m_a$ . The vertical lines denote our 3 sampling regions, discussed below. The mass fraction in the middle region is constrained to be  $\Omega_a/\Omega_d \lesssim 0.05$  at 95% confidence. Red regions show CMB-only constraints, while grey regions include large-scale structure data.

# SCALAR FIELD DARK MATTER

• .....

- **Halo Abundance and Assembly History with Extreme-Axion Wave Dark Matter at  $z \geq 4$** , Hsi-Yu Schive, Tzihong Chiueh. e-Print: arXiv:1706.03723 [astro-ph.CO].
- **Cosmological Perturbations of Extreme Axion in the Radiation Era**. Ui-Han Zhang, Tzihong Chiueh. e-Print: arXiv:1705.01439 [astro-ph.CO]
- **Cosmological signatures of ultra-light dark matter with an axion-like potential**. Francisco X. Linares Cedeño, Alma X. González-Morales, L. Arturo Ureña-López. e-Print: arXiv:1703.10180 [gr-qc]
- **The mass discrepancy-acceleration relation: a universal maximum dark matter acceleration and implications for the ultra-light scalar field dark matter model**, L. Arturo Ureña-López, Víctor H. Robles, T. Matos, e-Print: arXiv:1702.05103.
- **Cosmological production of ultralight dark matter axions**, Alberto Diez-Tejedor, David J. E. Marsh, e-Print: arXiv:1702.02116
- **On the hypothesis that cosmological dark matter is composed of ultra-light bosons, Lam Hui, Jeremiah P. Ostriker, Scott Tremaine, Edward Witten. Phys.Rev. D95 (2017) no.4, 043541. e-Print: arXiv:1610.08297.**
- **Simulations of solitonic core mergers in ultra-light axion dark matter cosmologies**, Bodo Schwabe, Jens C. Niemeyer, Jan F. Engels (Gottingen U.). e-Print: arXiv:1606.05151.
- **Contrasting Galaxy Formation from Quantum Wave Dark Matter**. Hsi-Yu Schive, Tzihong Chiueh, Tom Broadhurst, Kuan-Wei Huang. Astrophys.J. 818 (2016) no.1, 89
- **Towards accurate cosmological predictions for rapidly oscillating scalar fields as dark matter**, L. Arturo Ureña-López, Alma X. Gonzalez-Morales. e-Print: arXiv:1511.08195.
- **On wave dark matter in spiral and barred galaxies**. Luis A. Martinez-Medina, Hubert L. Bray, Tonatiuh Matos, JCAP 1512 (2015) no.12, 025. e-Print: arXiv:1505.07154
- **Cosmic Structure as the Quantum Interference of a Coherent Dark Wave**. Hsi-Yu Schive, Tzihong Chiueh, Tom Broadhurst. e-Print: arXiv:1406.6586 [astro-ph.GA]

• .....

# ONE SINGLE PARAMETER: MASS

$$\partial_{\mu}(g^{\mu\nu}\partial_{\nu}\phi) - m^2\phi = 0$$

# EQUATIONS OF MOTION: BACKGROUND (ORIGINAL)

$$H^2 = \frac{\kappa^2}{3} \left( \sum_I \rho_I + \rho_\phi \right), \quad (2.1a)$$

$$\dot{H} = -\frac{\kappa^2}{2} \left[ \sum_I (\rho_I + p_I) + (\rho_\phi + p_\phi) \right], \quad (2.1b)$$

$$\dot{\rho}_I = -3H(\rho_I + p_I), \quad (2.1c)$$

$$\ddot{\phi} = -3H\dot{\phi} - m^2\phi, \quad (2.1d)$$

where  $\kappa^2 = 8\pi G$ , a dot denotes derivative with respect to cosmic time  $t$ , and  $H$  is the Hubble parameter. The scalar field energy density  $\rho_\phi$  and pressure  $p_\phi$  are given by the known expressions:

$$\rho_\phi = \frac{1}{2}\dot{\phi}^2 + \frac{1}{2}m^2\phi^2, \quad p_\phi = \frac{1}{2}\dot{\phi}^2 - \frac{1}{2}m^2\phi^2. \quad (2.2)$$

# EQUATIONS OF MOTION: BACKGROUND (TRANSFORMED)

$$\frac{\kappa\dot{\phi}}{\sqrt{6H}} \equiv \Omega_{\phi}^{1/2} \sin(\theta/2), \quad \frac{\kappa V^{1/2}}{\sqrt{3H}} \equiv \Omega_{\phi}^{1/2} \cos(\theta/2), \quad (3a)$$

$$y_1 \equiv -2 \sqrt{2} \frac{\partial_{\phi} V^{1/2}}{H}, \quad (3b)$$

simply given by

$$w_{\phi} \equiv \frac{p_{\phi}}{\rho_{\phi}} = \frac{x^2 - y^2}{x^2 + y^2} = -\cos \theta. \quad (2.6)$$

That is, the new angular variable  $\theta$  is directly related to the scalar field EoS.

After some straightforward algebra, the KG equation (2.1d) becomes:

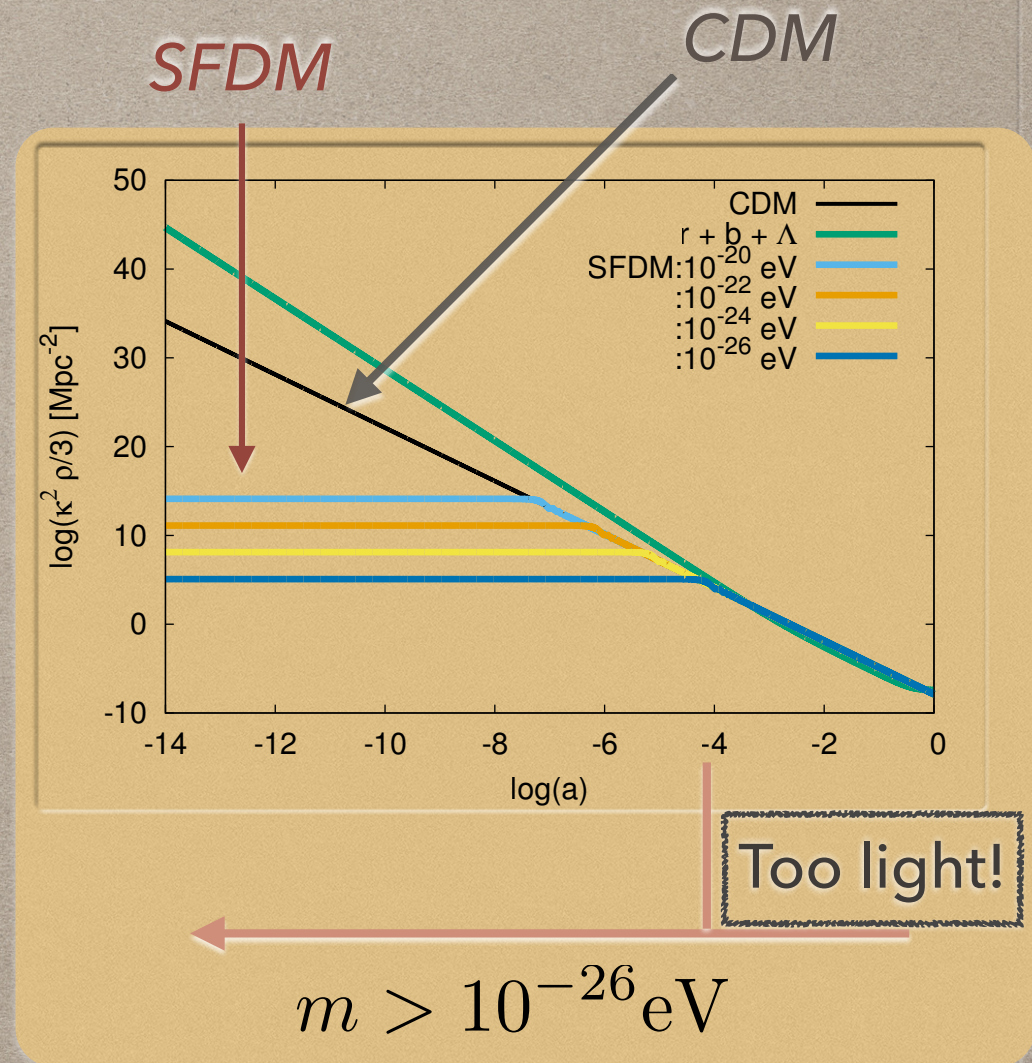
$$\theta' = -3 \sin \theta + y_1, \quad (2.7a)$$

$$y_1' = \frac{3}{2} (1 + w_{tot}) y_1, \quad (2.7b)$$

$$\Omega'_{\phi} = 3(w_{tot} - w_{\phi})\Omega_{\phi}. \quad (2.7c)$$

# SFDM: HOMOGENEOUS

- **SFDM redshifts as CDM** once in the regime of fast oscillations:
- This is a general output for any scalar field potential with a quadratic minimum
- The amplitude of the field has to be tuned to match CDM



U-L, González-Morales, JCAP 1607 (2016) 07, 048, arXiv:1511.08195

Matos, U-L, Phys.Rev.D 63 (2001) 063506

Sahni, Wang, Phys.Rev.D 62 (2000) 103517

# EQUATIONS OF MOTION: LINEAR PERTURBATIONS

$$\ddot{\varphi} = -3H\dot{\varphi} - (k^2/a^2 + m^2)\varphi - \frac{1}{2}\dot{\phi}\dot{h}, \quad (3.1)$$

where  $h$  is the trace of scalar metric perturbations (with  $\dot{h}$  known as the metric continuity), and  $k$  is a comoving wavenumber. The perturbations in density  $\delta\rho_\phi$ , pressure  $\delta p_\phi$ , and velocity divergence  $\Theta_\phi$ , are given, respectively, by [71, 72, 75]:

$$\delta\rho_\phi = \dot{\phi}\dot{\varphi} + \partial_\phi V \varphi, \quad (3.2a)$$

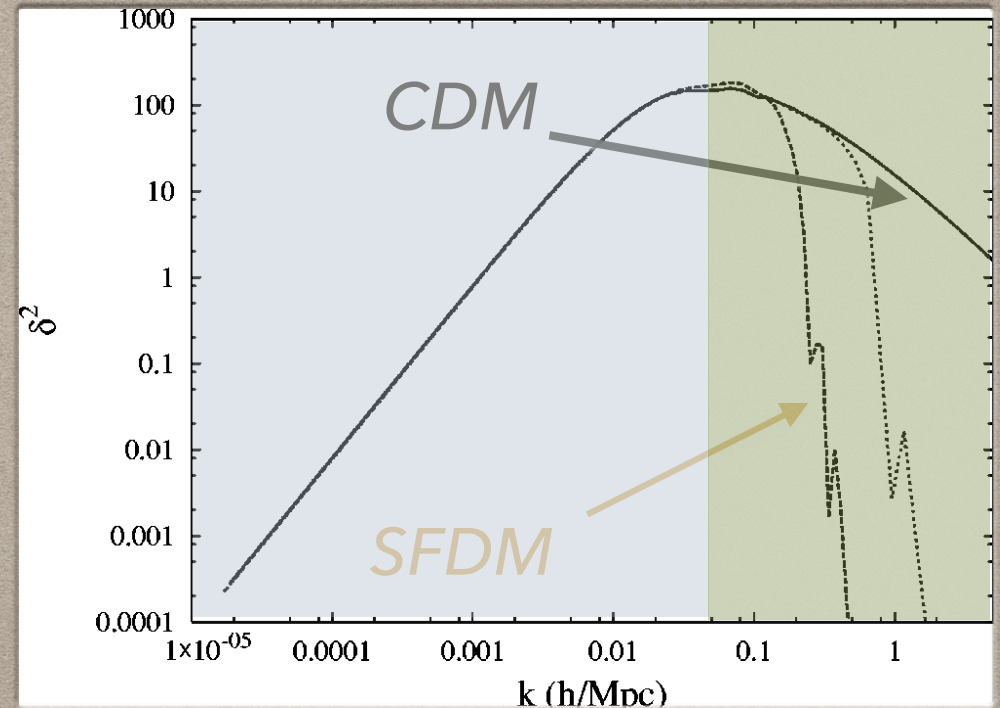
$$\delta p_\phi = \dot{\phi}\dot{\varphi} - \partial_\phi V \varphi, \quad (3.2b)$$

$$(\rho_\phi + p_\phi)\Theta_\phi = (k^2/a)\dot{\phi}\varphi. \quad (3.2c)$$

$$\begin{aligned} \delta'_0 &= \left[ -3 \sin \theta - \frac{k^2}{k_J^2} (1 - \cos \theta) \right] \delta_1 + \frac{k^2}{k_J^2} \sin \theta \delta_0 \\ &\quad - \frac{\bar{h}'}{2} (1 - \cos \theta), \\ \delta'_1 &= \left[ -3 \cos \theta - \frac{k^2}{k_J^2} \sin \theta + \frac{\lambda \Omega_\phi}{2y_1} \sin \theta \right] \delta_1 \\ &\quad + \left( \frac{k^2}{k_J^2} - \frac{\lambda \Omega_\phi}{2y_1} \right) (1 + \cos \theta) \delta_0 - \frac{\bar{h}'}{2} \sin \theta, \end{aligned}$$

# SFDM: INHOMOGENEOUS

- Initial conditions are the same as CDM at the end of inflation
- SFDM mimics the behaviour of CDM in linear perturbations at large scales
- SFDM has a sharp cut-off in the power spectrum at small scales



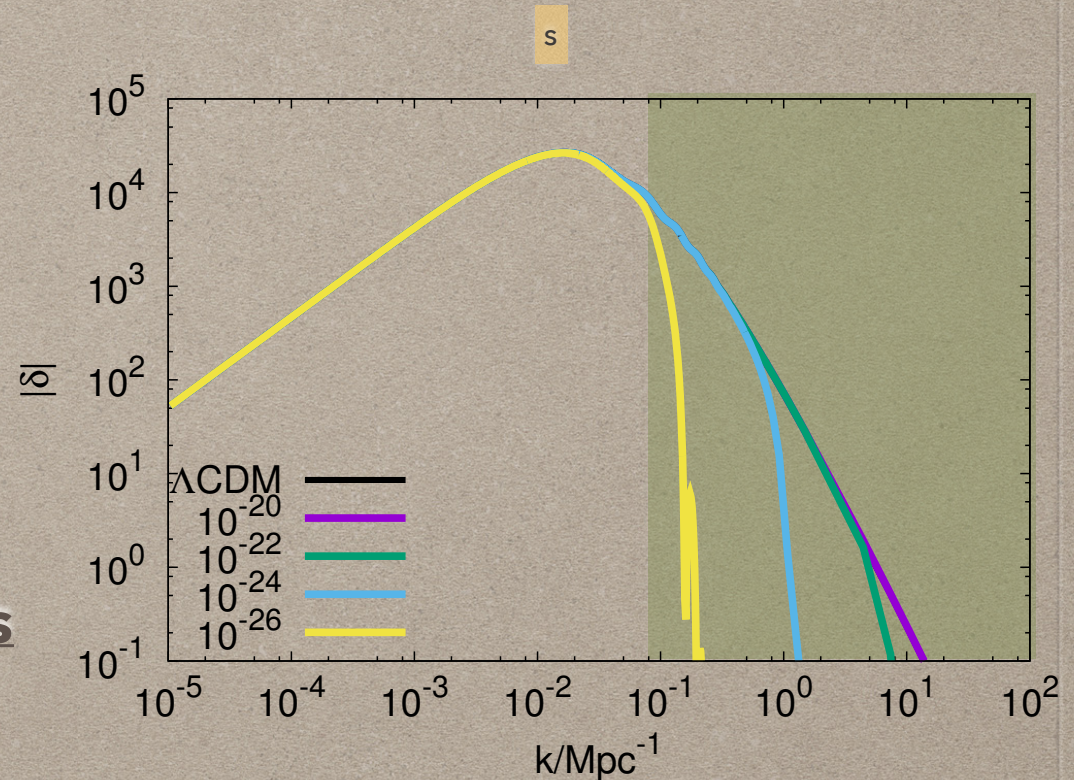
Power spectrum obtained by running **CMBFAST** up to  $z=50$

Matos, U-L, Phys.Rev. D63 (2001) 063506

# SFDM: INHOMOGENEOUS

- Initial conditions are the same as CDM at the end of inflation
- SFDM mimics the behaviour of CDM in linear perturbations at large scales
- SFDM has a sharp cut-off in the power spectrum at small scales
- The cut-off power spectrum is approximately given by:

$$P_\phi(k) \simeq \left[ \frac{\cos(x^3)}{1+x^8} \right]^2 P_{\text{CDM}}(k), \quad x \equiv k/k_{\text{cut}}$$



Power spectrum obtained by running **CLASS** up to  $z=0$

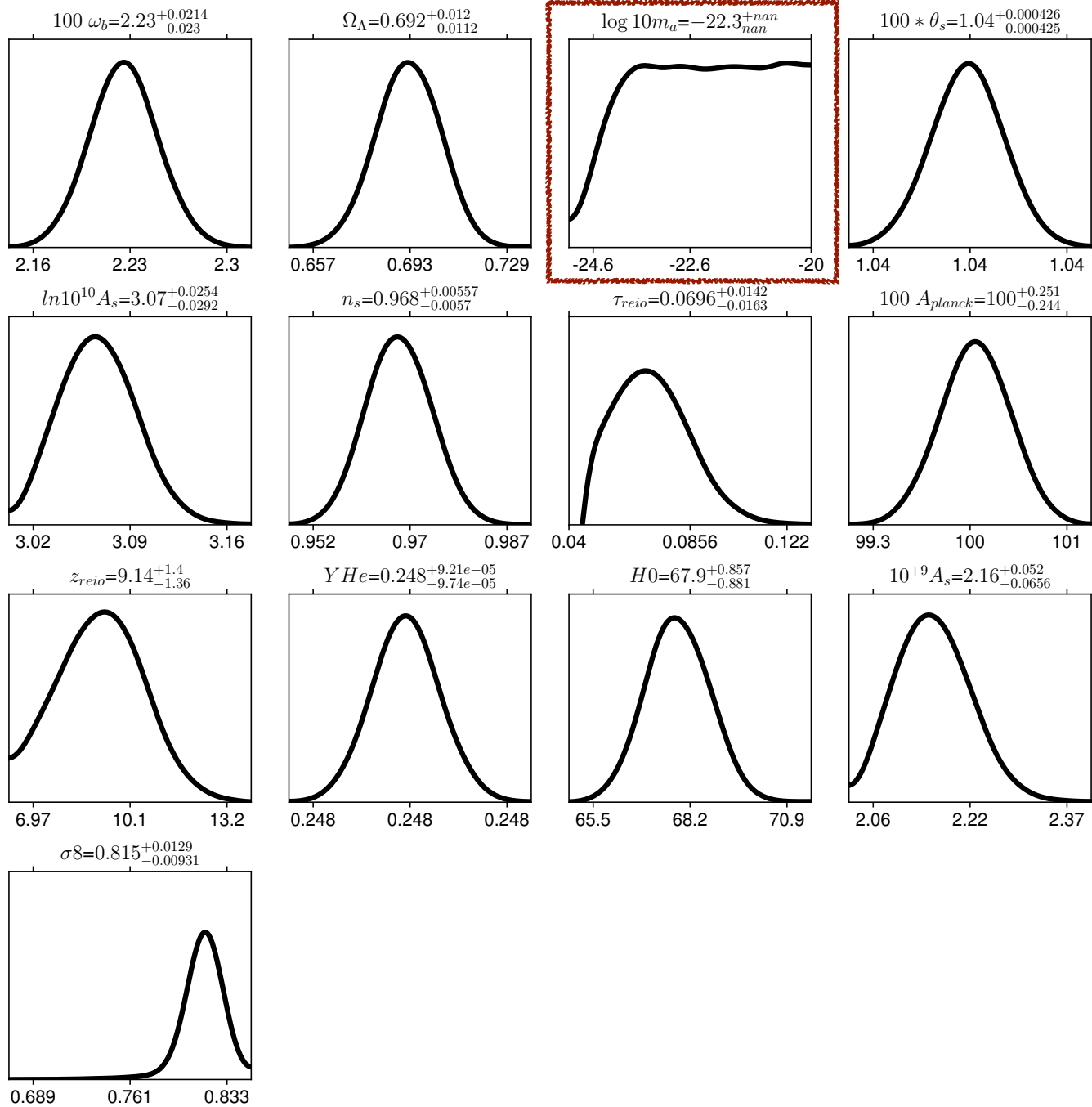


Figure courtesy  
Alma Gonzalez-  
Morales

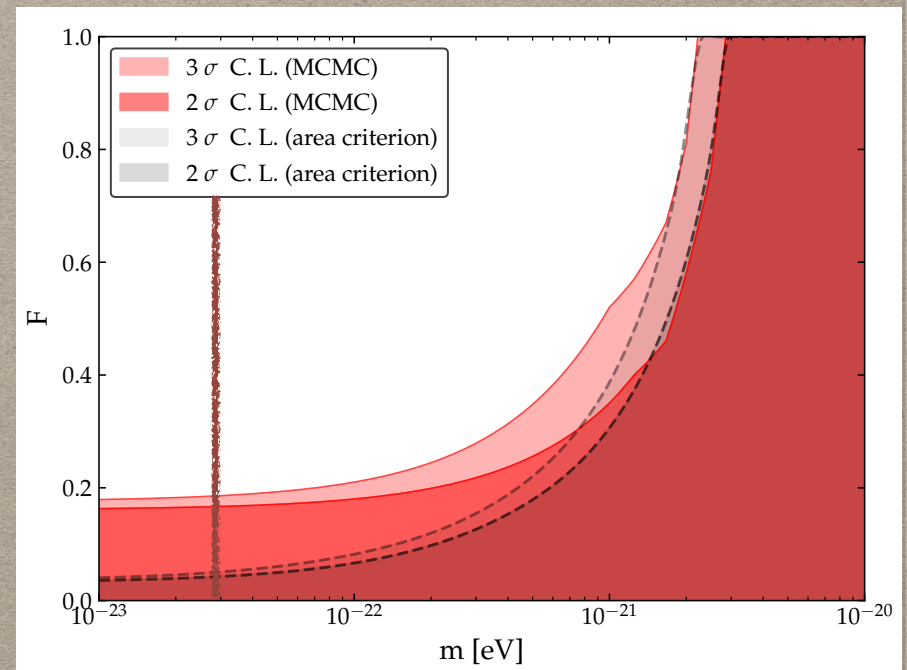
# Lyman-alpha forest

- 1D power spectrum calculated from the 3D linear power spectrum
- The observable is the 1D flux power spectrum, which is closely related to the 1D power spectrum
- Constraints from Lyman-alpha forest to the dark matter contribution of the scalar field.  $F$  represents the fractional dark matter contribution

Kobayashi et al, e-Print: arXiv:1708.00015

$$P_{1D}(k) = \frac{1}{2\pi} \int_k^\infty dk' k' P(k'),$$

$$P_F(k, z) = b^2(k, z) P_{1D}^{\text{linear}}(k, z)$$



# Lyman-alpha forest

An accurate calculation of the number of substructures  $N_{\text{sub}}$  with ultralight scalar DM would require high-resolution  $N$ -body simulations, which is beyond the scope of this paper. Here we instead make a rough estimate of  $N_{\text{sub}}$  using the following analytical expression for the number of subhalos,

$$\frac{dN_{\text{sub}}}{dM_{\text{sub}}} = \frac{1}{44.5} \frac{1}{6\pi^2} \frac{M_{\text{halo}}}{M_{\text{sub}}^2} \frac{P(1/R_{\text{sub}})}{R_{\text{sub}}^3 \sqrt{2\pi(S_{\text{sub}} - S_{\text{halo}})}}, \quad (4.1)$$

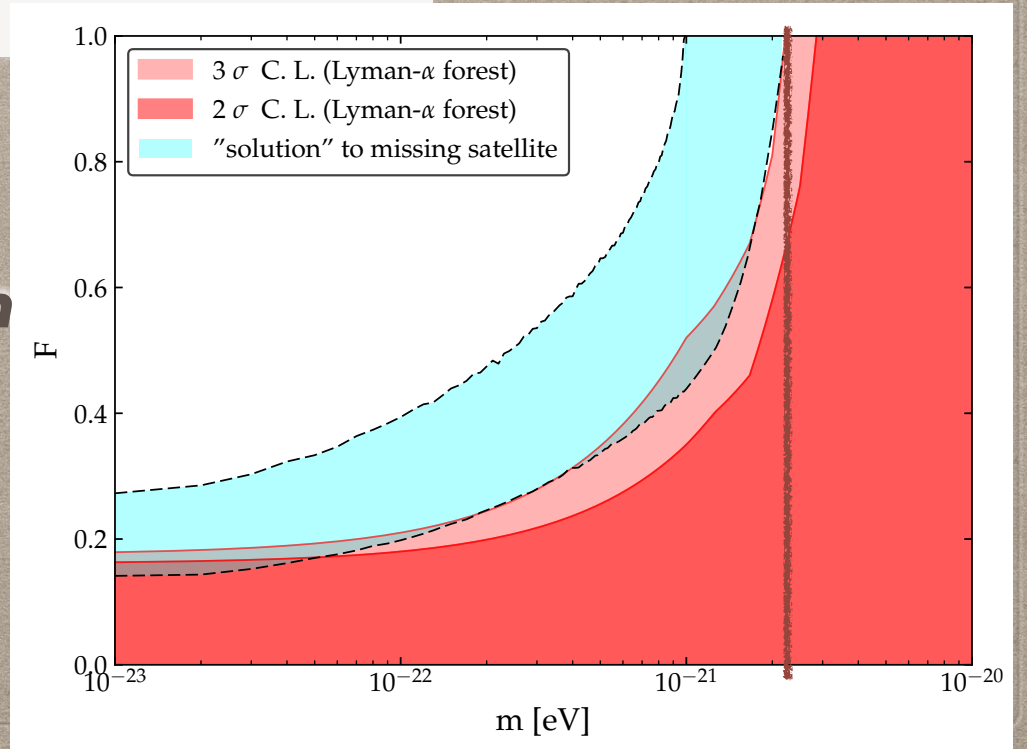
which was introduced in [51, 52] based on the conditional mass function normalized to the  $N$ -body simulation results.<sup>6</sup> Here  $R_{\text{sub}}$ ,  $M_{\text{sub}}$  and  $S_{\text{sub}}$  are radius, mass and variance of a given subhalo, while  $M_{\text{halo}}$  and  $S_{\text{halo}}$  are the mass and the variance of the main halo, defined as follows:

$$S_i = \frac{1}{2\pi^2} \int_0^{1/R_i} dk k^2 P(k), \quad M_i = \frac{4\pi}{3} \Omega_m \rho_c (cR_i)^3, \quad c = 2.5, \quad (4.2)$$

with  $P(k)$  being the linear power spectrum of a given model computed at redshift  $z = 0$ , and  $\rho_c$  the critical density today.

**The SFDM cannot be the DM  
and solve the missing problem  
at the same time!**

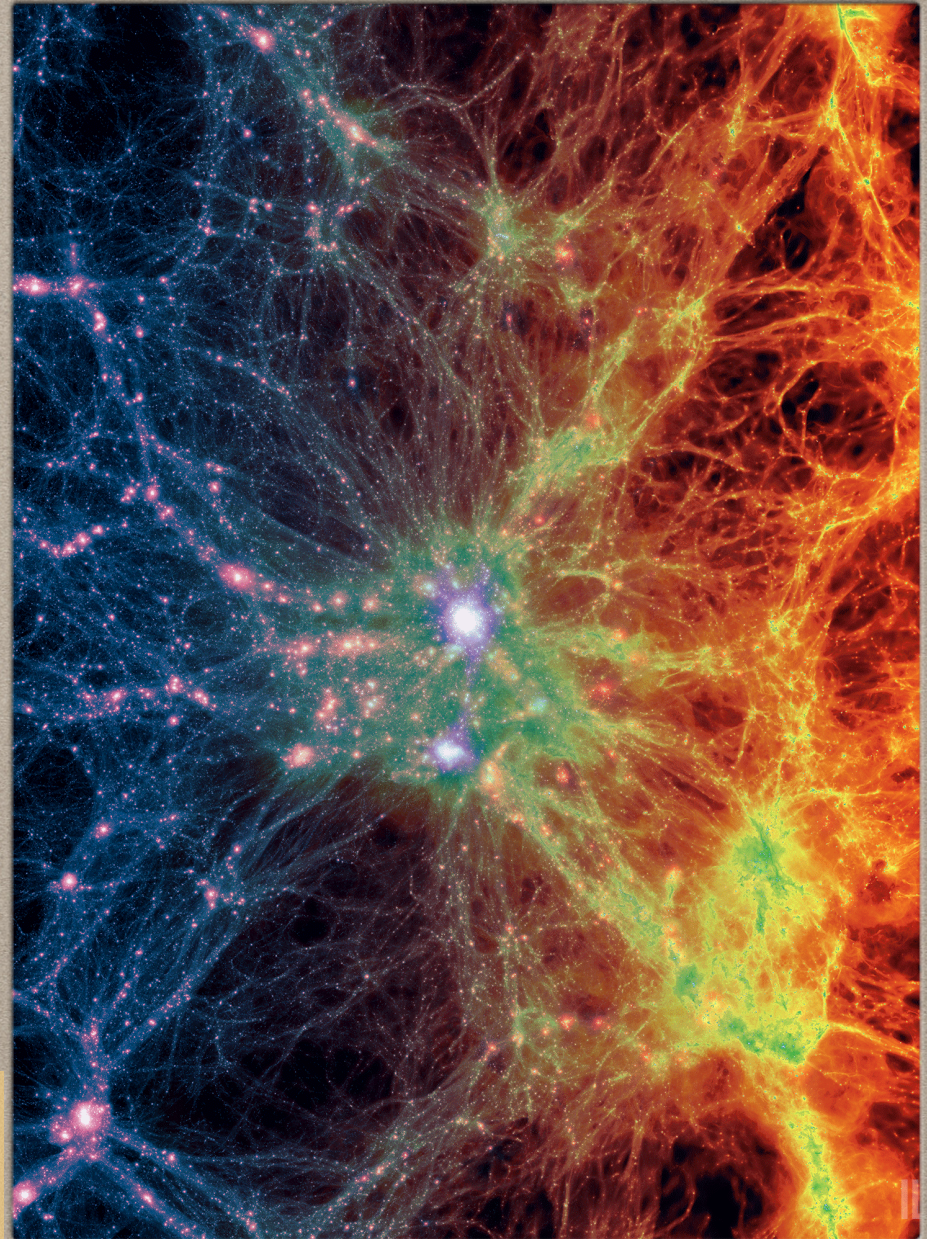
Kobayashi et al, e-Print: arXiv:1708.00015



# STRUCTURE FORMATION

## WHAT IS DARK MATTER?

Large scale projection through the Illustris volume at  $z=0$ ,  
centered on the most massive cluster, 15 Mpc/h deep.  
Shows dark matter density (left) transitioning to gas density (right).  
<http://www.illustris-project.org>



## HIGH-RESOLUTION SIMULATION ON STRUCTURE FORMATION WITH EXTREMELY LIGHT BOSONIC DARK MATTER

TAK-PONG WOO<sup>1,2</sup> AND TZIHONG CHIUH<sup>1,2,3</sup>

<sup>1</sup> Department of Physics, National Taiwan University, 106 Taipei, Taiwan; [bonwood@scu.edu.tw](mailto:bonwood@scu.edu.tw), [chiuehth@phys.ntu.edu.tw](mailto:chiuehth@phys.ntu.edu.tw)

<sup>2</sup> LeCosPa, National Taiwan University, 106 Taipei, Taiwan

<sup>3</sup> Center for Theoretical Sciences, National Taiwan University, 106 Taipei, Taiwan

Received 2008 June 2; accepted 2009 March 10; published 2009 May 5

### ABSTRACT

A bosonic dark matter model is examined in detail via high-resolution simulations. These bosons have particle mass of the order of  $10^{-22}$  eV and are noninteracting. If they do exist and can account for structure formation these bosons must be condensed into the Bose–Einstein state and described by a coherent wave function. This matter, also known as *fuzzy dark matter*, is speculated to be able, first, to eliminate the subgalactic halos to solve the problem of overabundance of dwarf galaxies, and, second, to produce flat halo cores in galaxies suggested by some observations. We investigate this model with simulations up to  $1024^3$  resolution in a  $1 h^{-1}$  Mpc box that maintains the background matter density  $\Omega_m = 0.3$  and  $\Omega_\Lambda = 0.7$ . Our results show that the extremely light bosonic dark matter can indeed eliminate low-mass halos through the suppression of short-wavelength fluctuations, as predicted by the linear perturbation theory. But in contrast to expectation, our simulations yield singular cores in the collapsed halos, where the halo density profile is similar, but not identical, to the Navarro–Frenk–White profile. Such a profile arises regardless of whether the halo forms through accretion or merger. In addition, the virialized halos exhibit anisotropic turbulence inside a well-defined virial boundary. Much like the velocity dispersion of standard dark matter particles, turbulence is dominated by the random radial flow in most part of the halos and becomes isotropic toward the halo cores. Consequently, the three-dimensional collapsed halo mass distribution can deviate from spherical symmetry, as the cold dark matter halo does.

*Key words:* dark matter – Galaxy: structure – large-scale structure of universe

*Online-only material:* color figures

## Newtonian version

The Lagrangian of nonrelativistic scalar field in the comoving frame is

$$L = \frac{a^3}{2} \left[ i\hbar \left( \psi^* \frac{\partial \psi}{\partial t} - \psi \frac{\partial \psi^*}{\partial t} \right) + \frac{\hbar^2}{a^2 m} (\nabla \psi)^2 - 2mV\psi^2 \right], \quad (3)$$

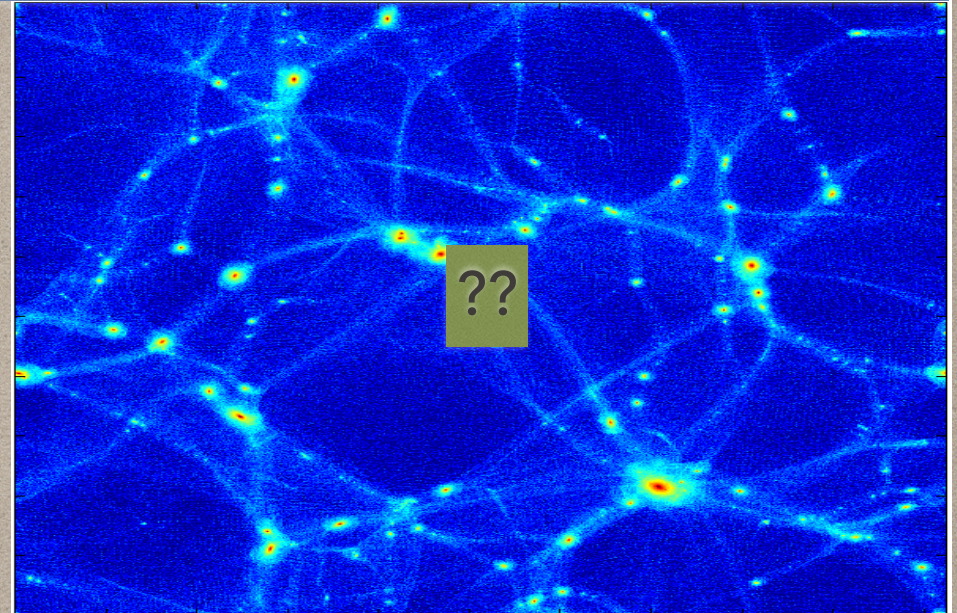
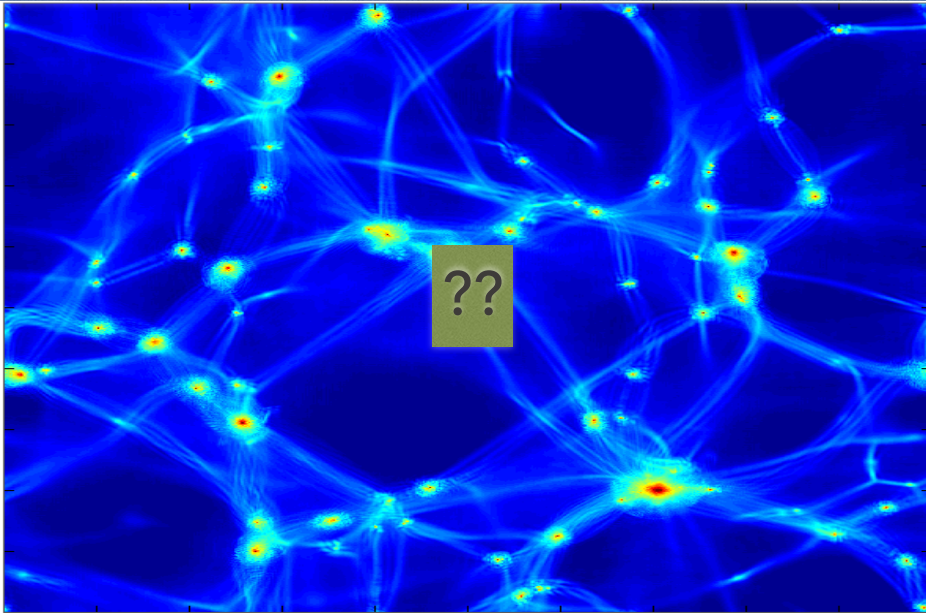
and the equation of motion for this Lagrangian gives a modified form of Schrödinger’s equation (Siddhartha & Uréna-López 2003):

$$i\hbar \frac{\partial \psi}{\partial t} = -\frac{\hbar^2}{2a^2 m} \nabla^2 \psi + mV\psi, \quad (4)$$

where  $\psi \equiv \phi(n_0/a^3)^{-1/2}$  with  $\phi$  being the ordinary wave function,  $n_0$  the present background number density, and  $V$  is the self-gravitational potential obeying the Poisson equation,

$$\nabla^2 V = 4\pi G a^2 \delta\rho = \frac{4\pi G}{a} \rho_0 (|\psi|^2 - 1). \quad (5)$$

# SFDM: INHOMOGENEOUS NON-LINEAR AND NON-RELATIVISTIC



Schive, Chiueh, Broadhurst, Nature Physics 10, 496-499 (2014)  
Schive et al, Phys.Rev.Lett. 113 (2014) no.26, 261302

# SFDM: INHOMOGENEOUS

## CDM & WAVE DARK MATTER

# SOLITON CORE

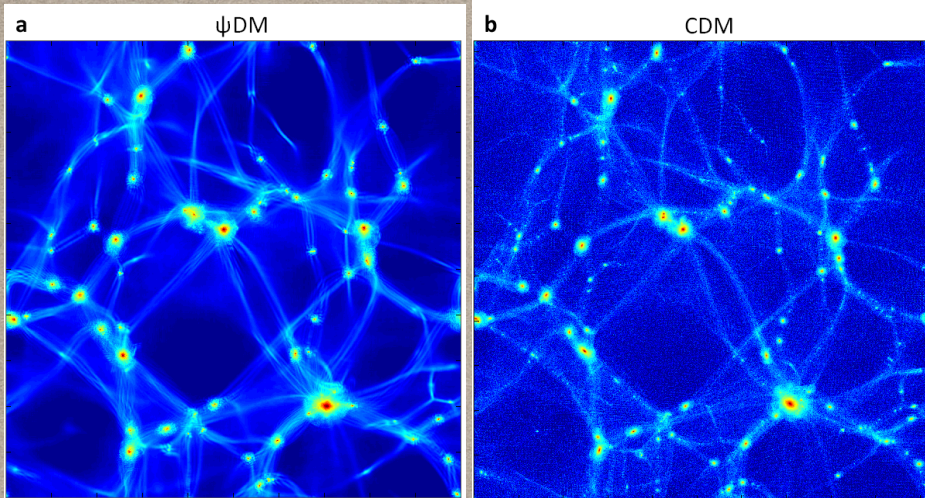


**Figure 1:** Comparison of cosmological large-scale structures formed by standard CDM and by wave-like dark matter,  $\psi$ DM. Panel (a) shows the structure created by evolving a single coherent wave function for  $\Lambda\psi$ DM calculated on AMR grids. Panel (b) is the structure simulated with a standard  $\Lambda$ CDM N-body code GADGET-2<sup>12</sup> for the same cosmological parameters, with the high-k modes of the linear power spectrum intentionally suppressed in a way similar to the  $\psi$ DM model to highlight the comparison of large-scale features. This comparison clearly demonstrates that the large scale distribution of filaments and voids is indistinguishable between these two completely different calculations, as desired given the success of  $\Lambda$ CDM in describing the observed large scale structure.  $\psi$ DM arises from the low momentum state of the condensate so that it is equivalent to collisionless CDM well above the Jeans scale.

$$m = 8 \times 10^{-23} \text{ eV}$$

## SFDM: INHOMOGENEOUS COMPARISON WITH CDM

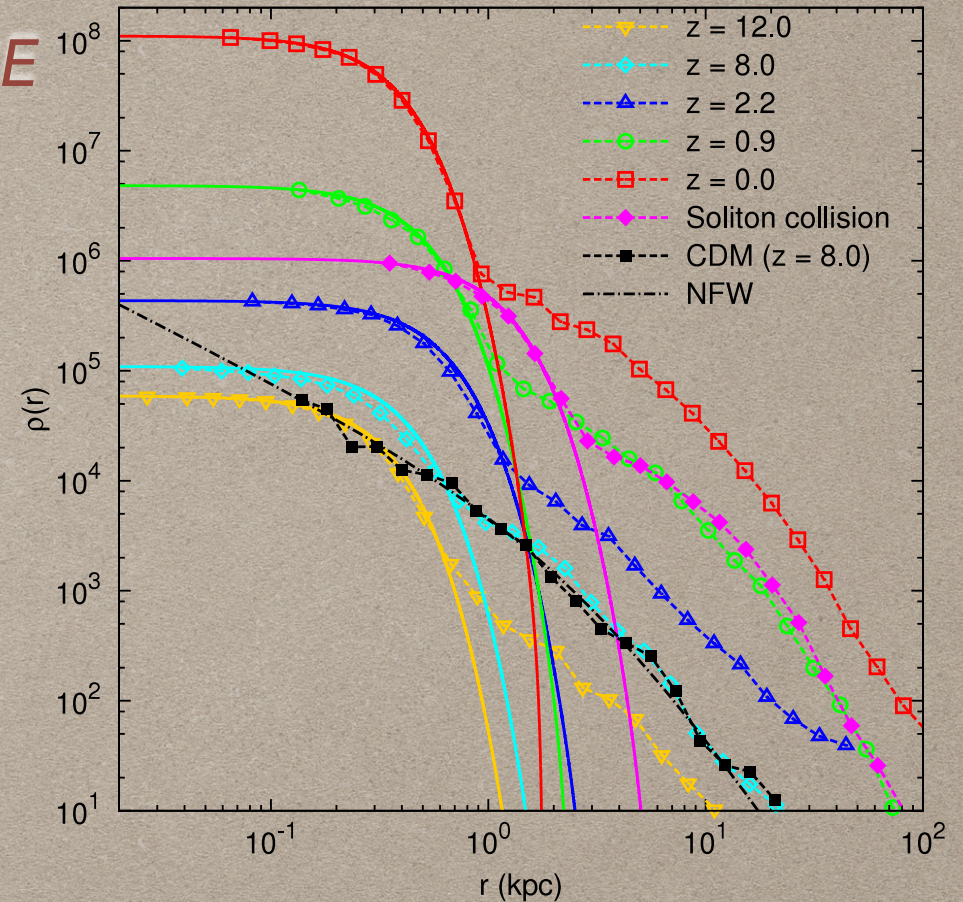


**FIG. 1:** Density profiles of  $\psi$ DM halos. Dashed lines with various opened symbols show five examples at different redshifts between  $12 \geq z \geq 0$ . The DM density is normalized to the cosmic background density. A distinct core forms in every halo as a gravitationally self-bound object, satisfying the redshift-dependent soliton solution (solid lines) upon proper  $\lambda$  scaling. Filled diamonds show an example from the soliton collision simulations renormalized to the comoving coordinates at  $z = 0$ . The same  $z = 8$  halo in a CDM simulation (filled squares) fit by an NFW profile (dot-dashed line) is also shown for comparison.

# SOLITON CORE

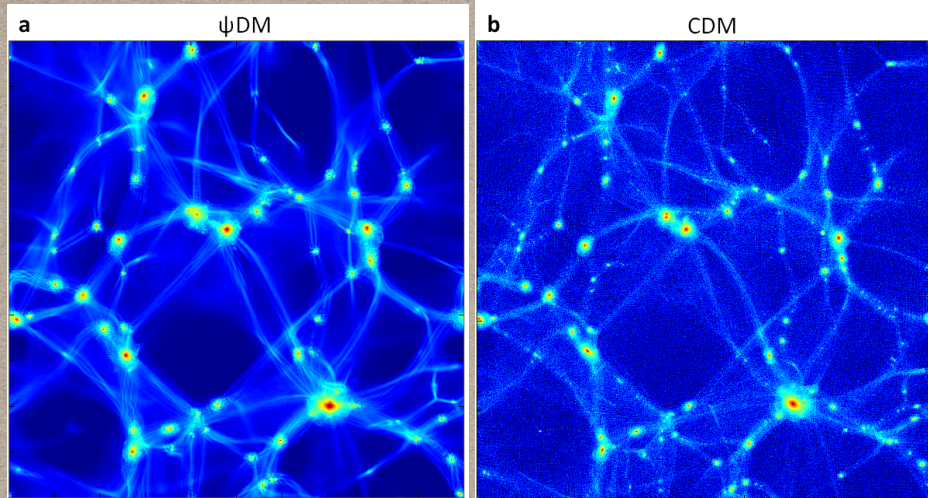


**Figure 1:** Comparison of cosmological large-scale structures formed by standard CDM and by wave-like dark matter,  $\psi$ DM. Panel (a) shows the structure created by evolving a single coherent wave function for  $\Lambda\psi$ DM calculated on AMR grids. Panel (b) is the structure simulated with a standard  $\Lambda$ CDM N-body code GADGET-2<sup>12</sup> for the same cosmological parameters, with the high-k modes of the linear power spectrum intentionally suppressed in a way similar to the  $\psi$ DM model to highlight the comparison of large-scale features. This comparison clearly demonstrates that the large scale distribution of filaments and voids is indistinguishable between these two completely different calculations, as desired given the success of  $\Lambda$ CDM in describing the observed large scale structure.  $\psi$ DM arises from the low momentum state of the condensate so that it is equivalent to collisionless CDM well above the Jeans scale.

$$m = 8 \times 10^{-23} \text{ eV}$$

## SFDM: INHOMOGENEOUS COMPARISON WITH CDM

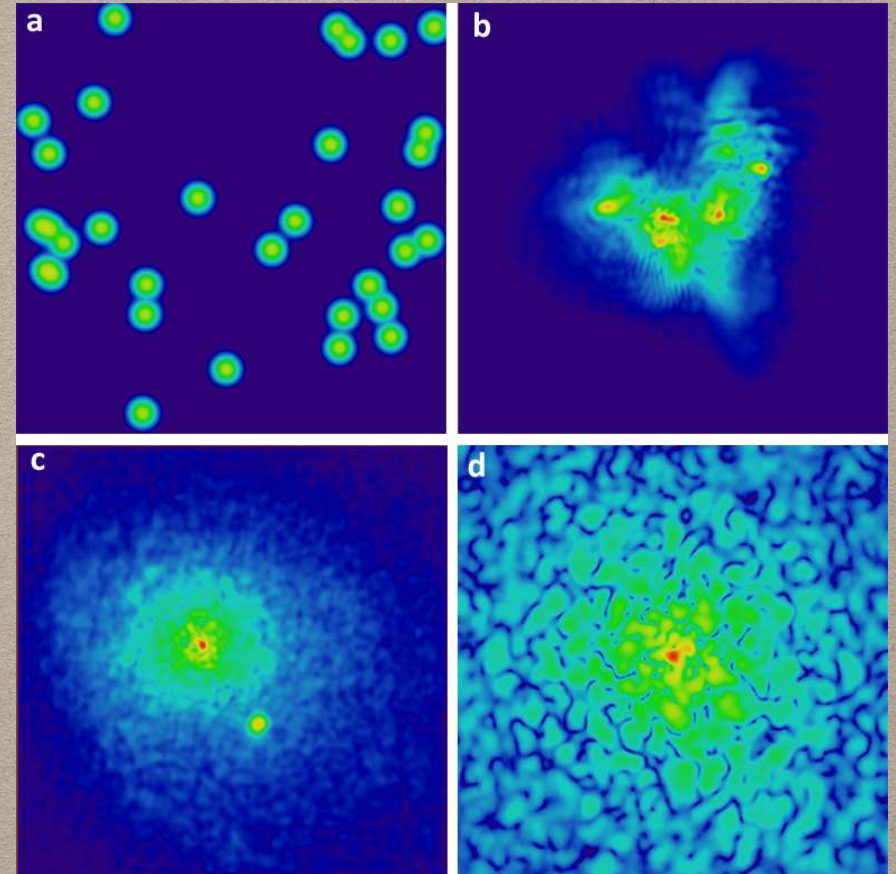
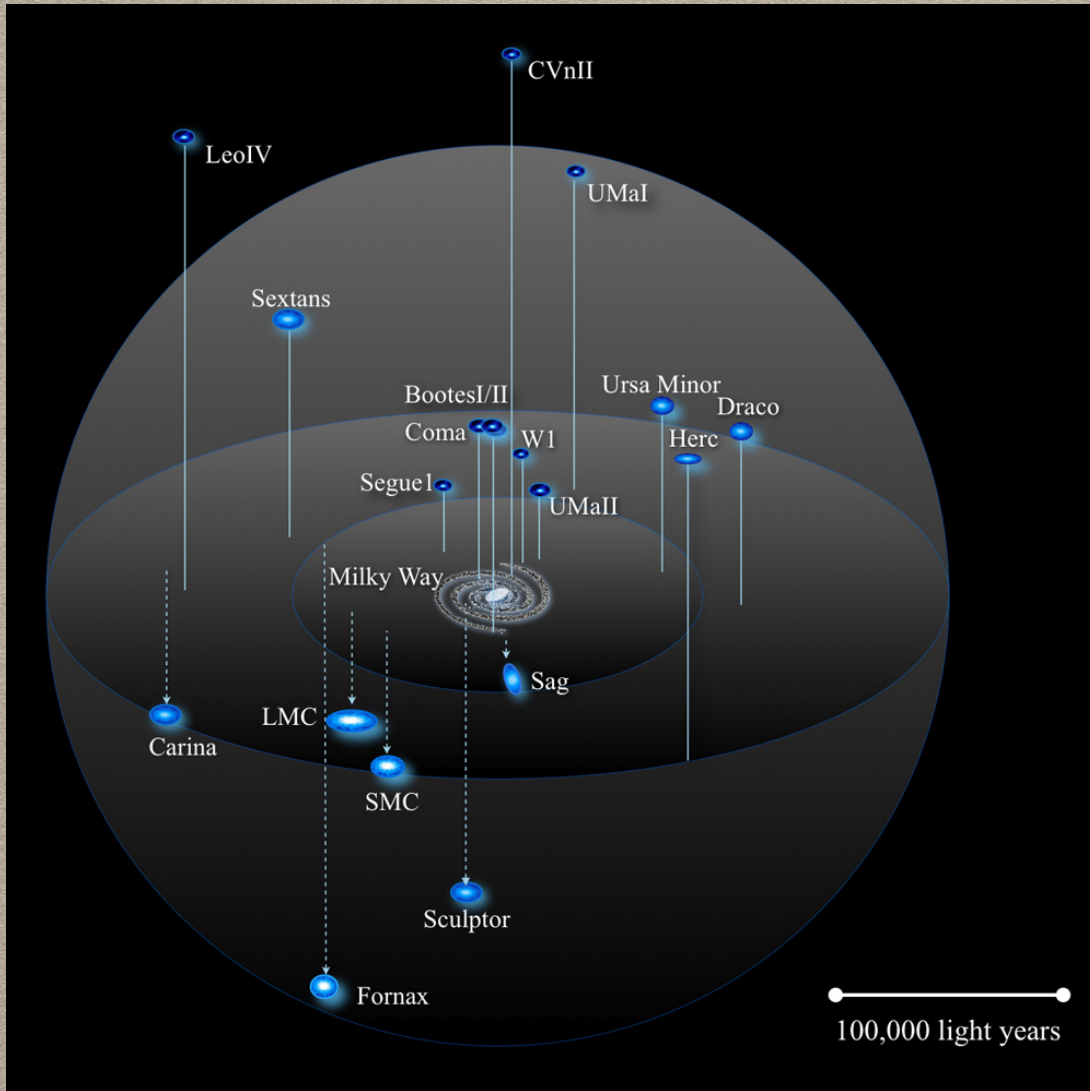


**FIG. 3:** Snapshots of a soliton collision simulation. Panels (a)-(c) show the projected density distribution at the initial and intermediate stages, and panel (d) shows a close-up of the conspicuous solitonic core at the final stage. Fluctuating density granules resulting from the quantum wave interference appear everywhere and have a size similar to the central soliton.

Schive et al, Phys.Rev.Lett. 113 (2014) no.26, 261302  
e-Print: arXiv:1407.7762



$$\rho(r) = \frac{\rho_s}{(1 + r^2/r_s^2)^8}$$

$$r_{\text{sol}} = \left[ \frac{\rho_{\text{sol}}}{2.42 \times 10^9 M_{\odot} \text{kpc}^{-3}} \left( \frac{m_a}{10^{-22} \text{eV}} \right)^2 \right]^{-0.25} \text{kpc}.$$

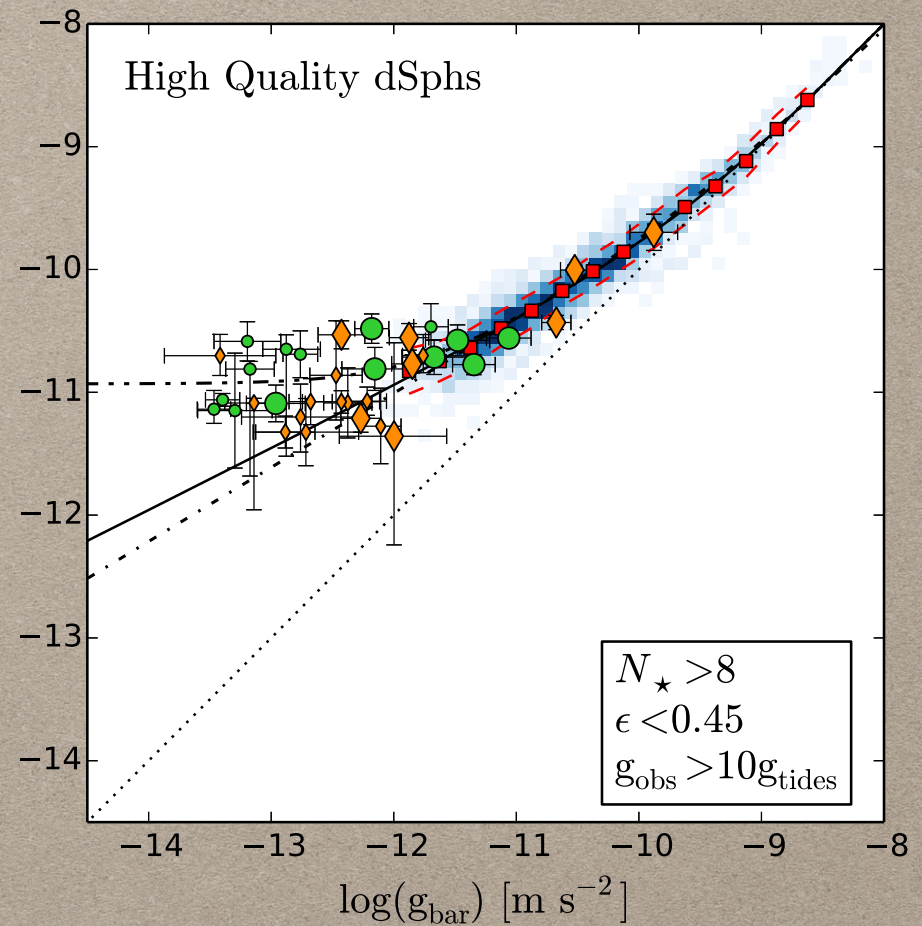
# COMPARISON AT SMALL SCALES

# THE MASS-ACCELERATION DISCREPANCY RELATION

- The rotation curves of galaxies seem to follow a **simple law** regarding the gravitational accelerations
- The new law seems to agree with a **MOND-ian** point of view

$$g_{\text{obs}} = \mathcal{F}(g_{\text{bar}}) = \frac{g_{\text{bar}}}{1 - e^{-\sqrt{g_{\text{bar}}/g_{\ddagger}}}}, \quad (11)$$

where the only free parameter is  $g_{\ddagger}$ . For  $g_{\text{bar}} \gg g_{\ddagger}$ , Equation (11) gives  $g_{\text{obs}} \simeq g_{\text{bar}}$ , in line with the values of  $\alpha$ ,  $\hat{g}_{\text{bar}}$ , and  $\hat{g}_{\text{obs}}$  found above. For  $g_{\text{bar}} \ll g_{\ddagger}$ , Equation (11) imposes a low-acceleration slope of 0.5. A slope of 0.5 actually provides a better fit to the low-acceleration data than 0.6 does (see Figure 3). We find  $g_{\ddagger} = (1.20 \pm 0.02) \times 10^{-10} \text{ m s}^{-2}$ .



Lelli et al, *Astrophys.J.* 836 (2017) no.2, 152

# THE MASS DISCREPANCY ACCELERATION RELATION

- The MDAR implies a **hidden degeneracy** for the free parameters of **any given density profile**
- In the case of WaveDM, there is a degeneracy between **the soliton radius** and **the boson mass**
- The MDAR also predicts a **constant surface density** for all density profiles
- For **WaveDM** we obtain:

$$\left(\frac{r_s}{\text{pc}}\right)^{-3} \left(\frac{m_a}{10^{-23}\text{eV}}\right)^{-2} = 4.1 \times 10^{-15} \left(\frac{\mu_{DM}}{M_\odot \text{pc}^{-2}}\right).$$

U-L, Robles, Matos, PRD 96 (2017) no.4, 043005, e-Print: arXiv:1702.05103

stars outside  $r_c$  to break this degeneracy. The mean correlation is found to be  $m_\psi \propto r_c^{-1.4}$ , shallower than the fully degenerate case. It explains the tendency that the tangen-

Chen, Schive, Chiueh, e-Print: arXiv:1606.09030

$$\mu_{DM} = \rho_s r_s = 648 M_\odot \text{pc}^{-2}$$

U-L, Robles, Matos, PRD 96 (2017) no.4, 043005, e-Print: arXiv:1702.05103

García-Aspeitia et al, e-Print: arXiv:1511.06740

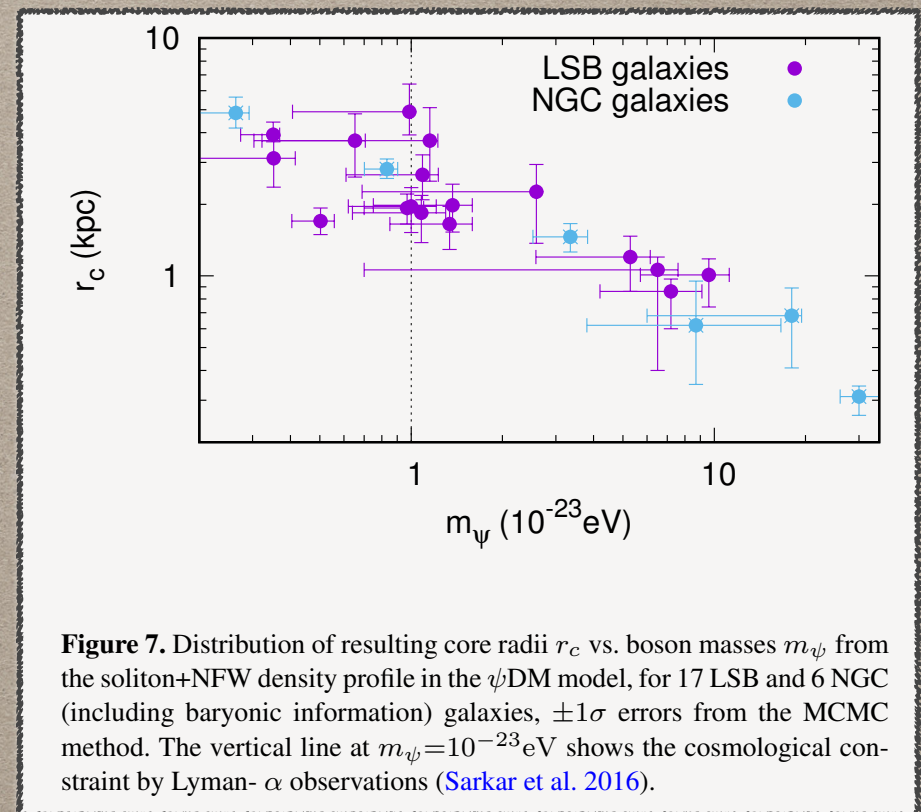
# THE HIDDEN DEGENERACY AT SMALL SCALES

- The parameters in the **density profile** are not independent, this comes from the properties of the **Schrodinger-Poisson system of equations**
- Fits to small scale structure **cannot fix the boson mass**, but just any combination of **two parameters**.
- Fits show a **strong correlation** between the **boson mass and the soliton radius**

Bernal, Fernández-Hernández, Matos, Rodriguez-Meza  
e-Print: arXiv:1701.00912

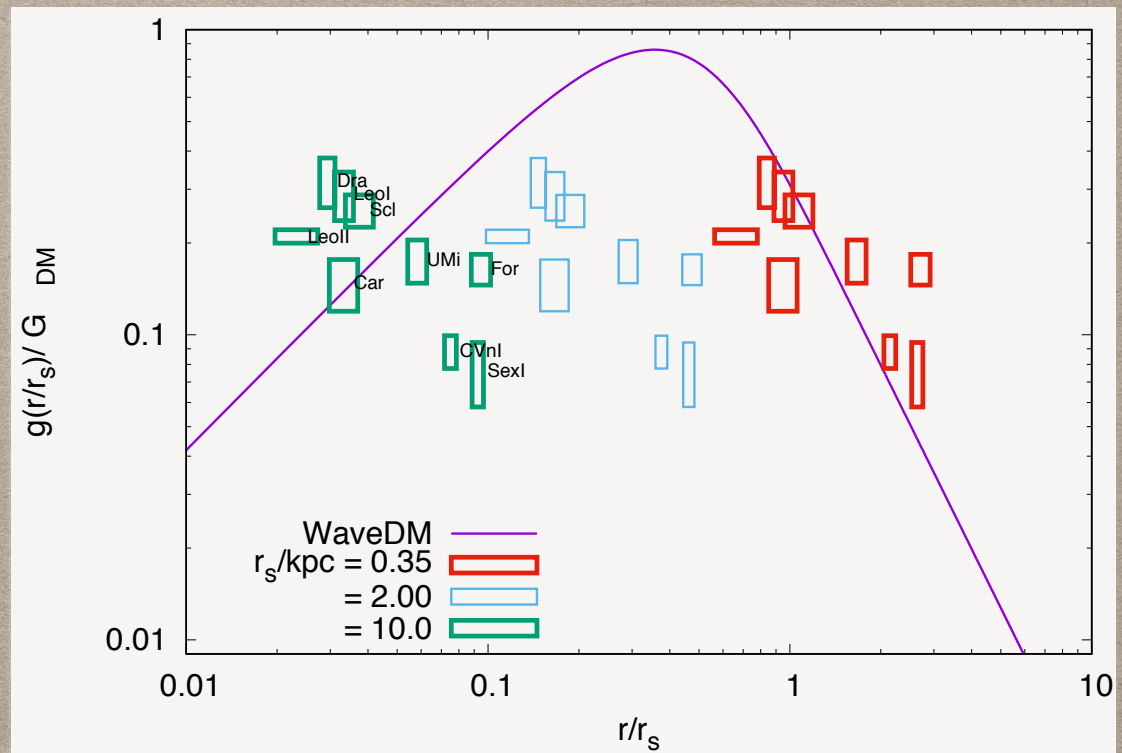
$$\rho(r) = \frac{\rho_s}{(1 + r^2/r_s^2)^8}$$

$$r_{\text{sol}} = \left[ \frac{\rho_{\text{sol}}}{2.42 \times 10^9 \text{ M}_\odot \text{ kpc}^{-3}} \left( \frac{m_a}{10^{-22} \text{ eV}} \right)^2 \right]^{-0.25} \text{ kpc}.$$



# BREAKING THE DEGENERACY

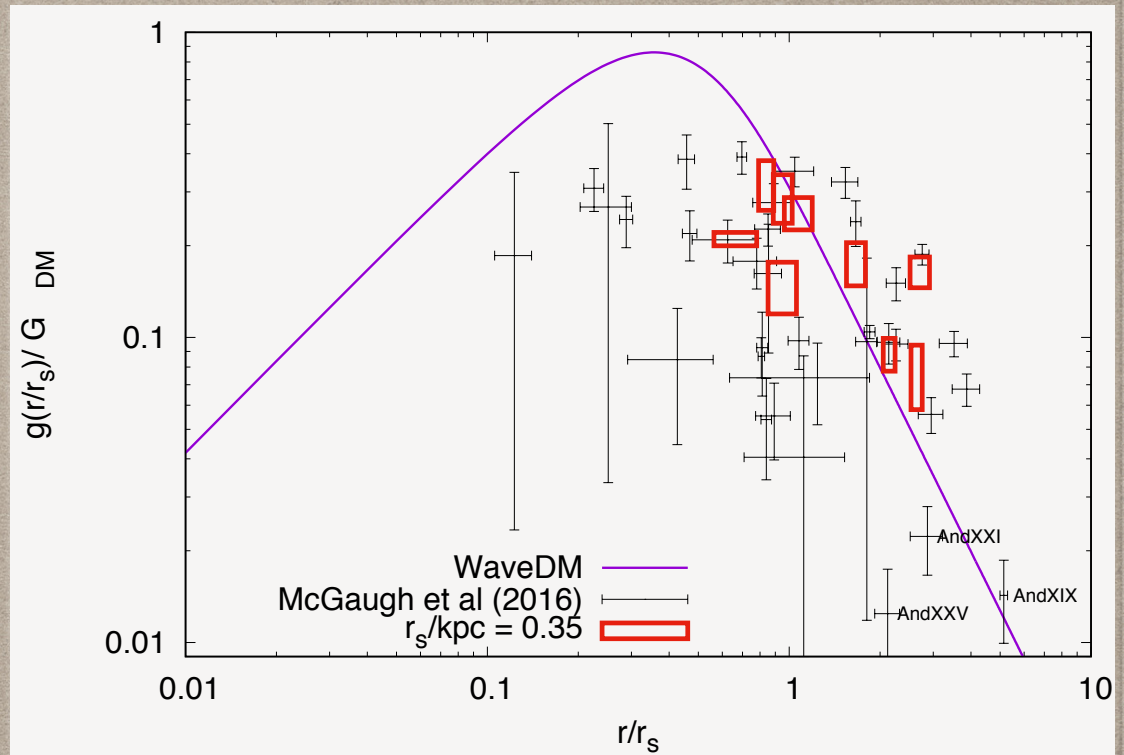
- Comparison of the gravity profile with data from **classical dSphs in the Milky Way**
- **The theoretical curve is normalized** with the surface density as suggested by the MDAR
- The data was obtained from Fattahi et al, arXiv:1607:06497
- Shown are three values of the soliton radius. The best option seems to be **0.30 kpc**



U-L, Robles, Matos, PRD 96 (2017) no.4, 043005, e-Print: arXiv:1702.05103

# BREAKING THE DEGENERACY

- Comparison of the gravity profile with data from **all dSphs in the Milky Way and Andromeda**
- The data was obtained from Fattahi et al, arXiv:1607:06497, and Lelli et al, Astrophys.J. 836 (2017) 2, 152
- The outliers **AndXIX, AndXXI and AndXXV** seem to follow the **downward trend** of the theoretical curve
- The boson mass is  **$10^{-21}$  eV**, the soliton radius is **300pc**, and the soliton mass is  **$10^7$  solar masses**



U-L, Robles, Matos, PRD 96 (2017) no.4, 043005, e-Print: arXiv:1702.05103

A common mass scale for satellite galaxies of the Milky Way  
Nature 454, 1096-1097 (28 August 2008)

Here we use new measurements of the velocities of the stars in these galaxies<sup>6,7</sup> to show that they are consistent with them having a common mass of about  $10^7$  within their central 300 parsecs. This result demonstrates that the faintest of the Milky Way satellites are the most dark-matter-dominated galaxies known, and could be a hint of a new scale in galaxy formation or a characteristic scale for the clustering of dark matter.

# BREAKING THE DEGENERACY

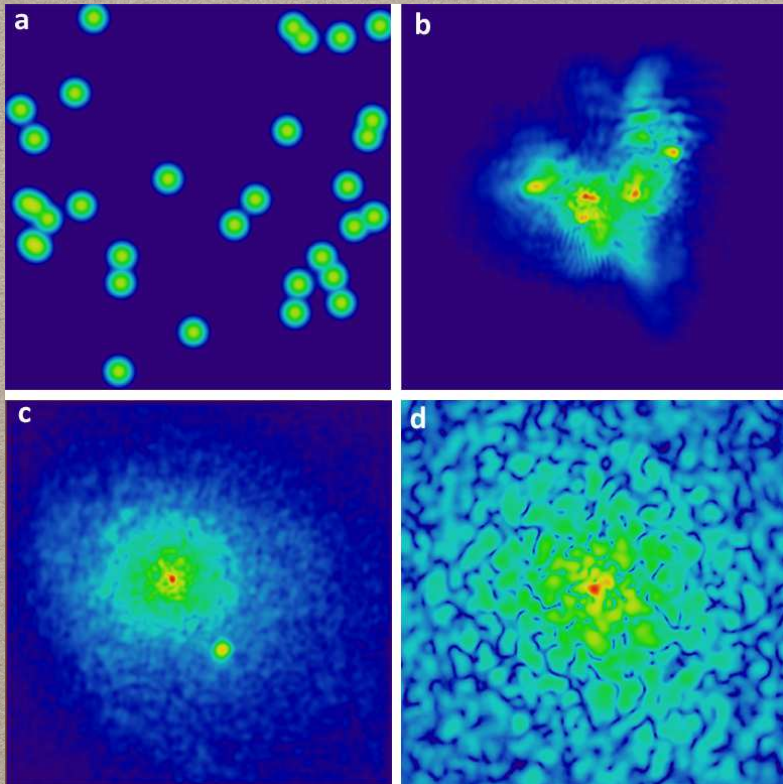
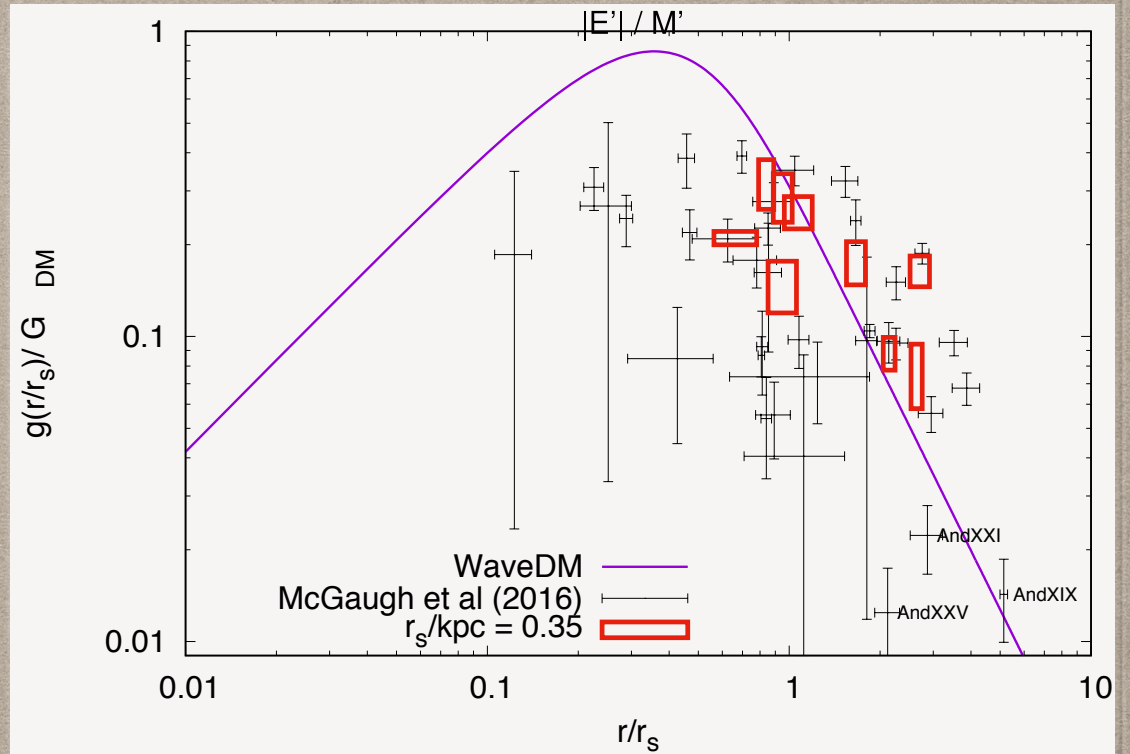


FIG. 3: Snapshots of a soliton collision simulation. Panels (a)-(c) show the projected density distribution at the initial and intermediate stages, and panel (d) shows a close-up of the conspicuous solitonic core at the final stage. Fluctuating density granules resulting from the quantum wave interference appear everywhere and have a size similar to the central soliton.

Schive et al, Phys.Rev.Lett. 113 (2014) no.26, 261302  
e-Print: arXiv:1407.7762



U-L, Robles, Matos, PRD 96 (2017) no.4, 043005, e-Print: arXiv:1702.05103

tion of the dense solitonic cores. A present-day galaxy with a typical halo mass of  $2 \times 10^{12} M_{\odot}$  will have  $M_c \sim 5 \times 10^8 M_{\odot}$  and  $r_c \sim 160$  pc. For a high-redshift

# ANOTHER SINGLE PARAMETER: QUARTIC SELF-INTERACTION

$$\partial_{\mu}(g^{\mu\nu}\partial_{\nu}\phi) - m^2 f^2 [1 - \cos(\phi/f)] = 0$$

# EXTREME-AXION MATTER

- It refers to the case in which the **axion decay constant**  $f$  is small enough.
- In cosmological simulations, it also means that initial **conditions are set up close to the maximum of the axion potential**.
- There are measurable effects in the background evolution and **the MPS**

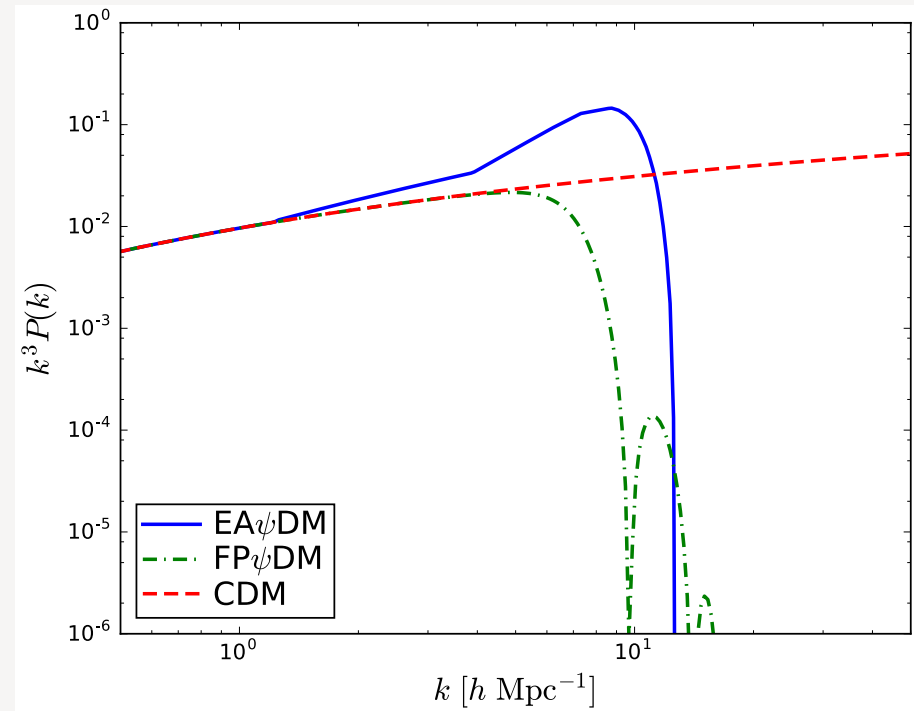


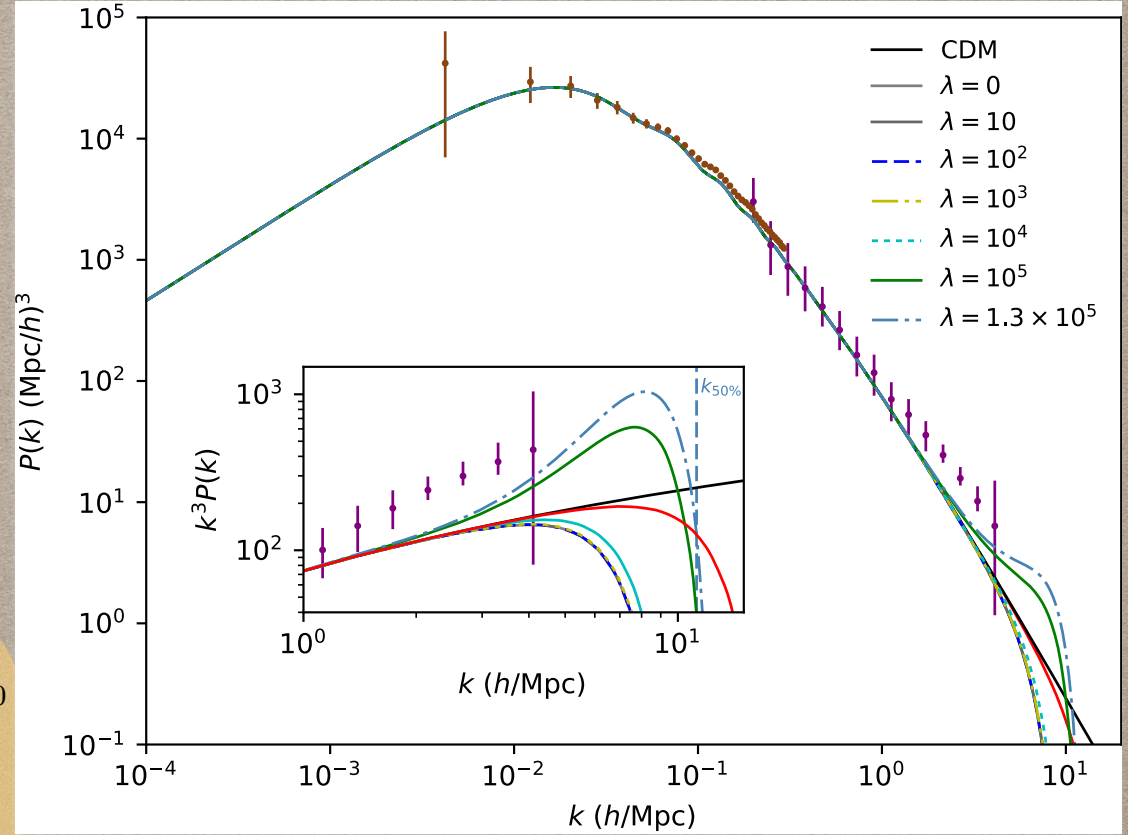
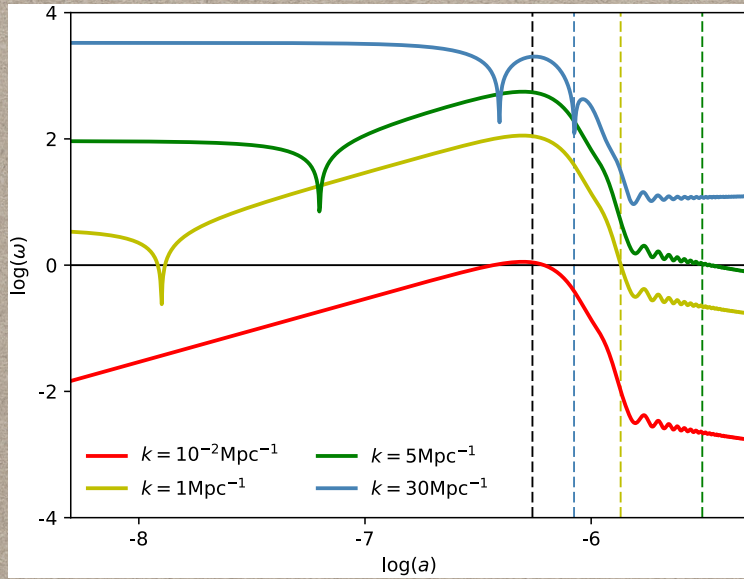
**Figure 1.** Linear power spectra of CDM, FP $\psi$ DM, and EA $\psi$ DM at  $z = 100$ . Both  $\psi$ DM power spectra feature a strong suppression at the high- $k$  end, while EA $\psi$ DM shows a broad spectral bump peaking at  $k \sim 8 h \text{ Mpc}^{-1}$  and a cut-off wavenumber roughly twice larger than that of FP $\psi$ DM.

Schive, Chiueh, e-Print: arXiv:1706.03723 [astro-ph.CO]

Zhang, Chiueh, PRD 96 (2017) no.6, 063522, e-Print: arXiv:1705.01439

Zhang, Chiueh, Phys.Rev. D96 (2017) no.2, 023507, e-Print: arXiv:1702.07065

# EXTREME-AXION MATTER



$$\delta'_0 = \left[ -3 \sin \theta - \frac{k^2}{k_J^2} (1 - \cos \theta) \right] \delta_1 + \frac{k^2}{k_J^2} \sin \theta \delta_0 - \frac{\bar{h}'}{2} (1 - \cos \theta),$$

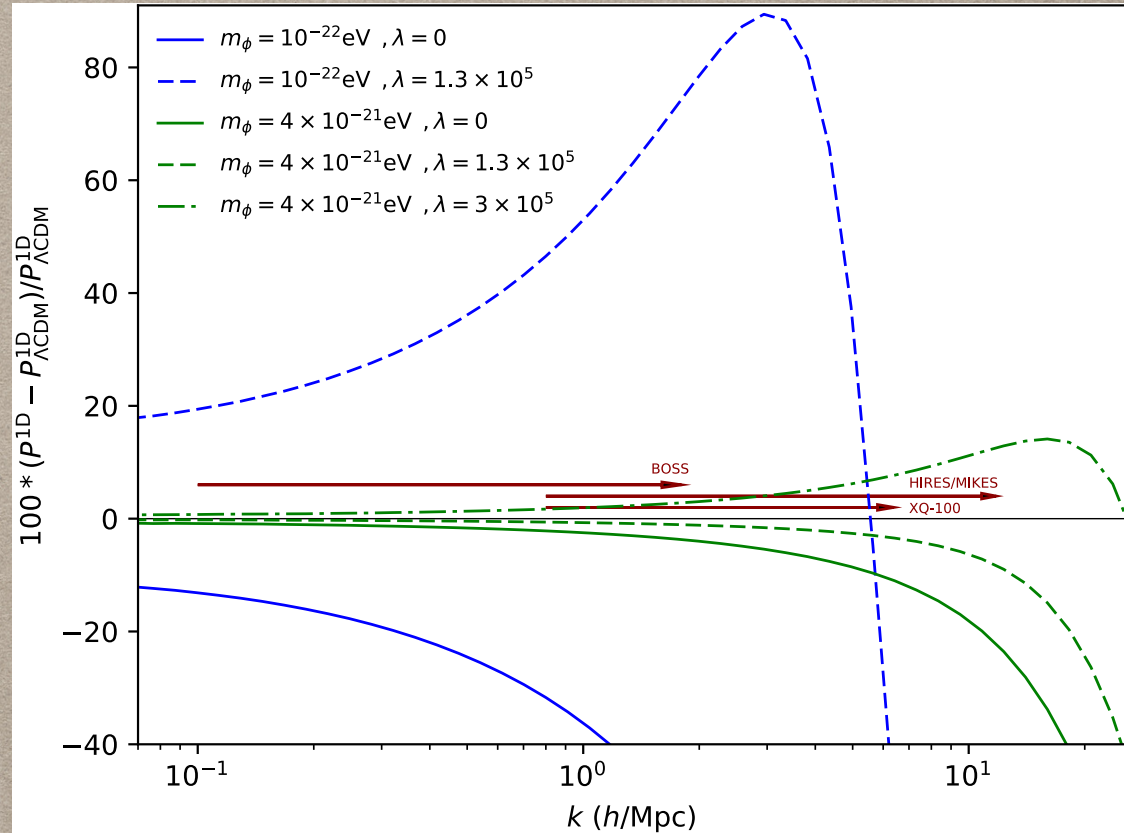
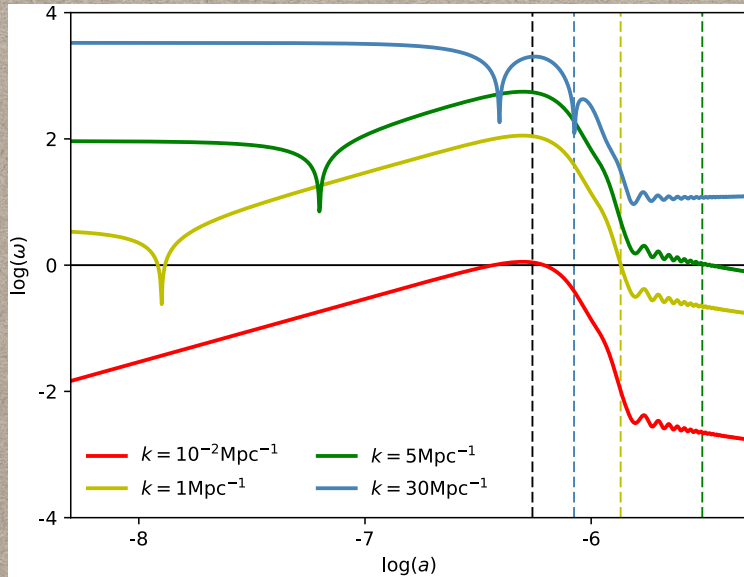
$$\delta'_1 = \left[ -3 \cos \theta - \frac{k^2}{k_J^2} \sin \theta + \frac{\lambda \Omega_\phi}{2y_1} \sin \theta \right] \delta_1 + \left( \frac{k^2}{k_J^2} - \frac{\lambda \Omega_\phi}{2y_1} \right) (1 + \cos \theta) \delta_0 - \frac{\bar{h}'}{2} \sin \theta,$$

$$\lambda = 3 / (8\pi G f^2)$$

Tachyonic effect

Linares, Gonzalez-Morales, U-L, PRD96 (2017) no.6, 061301, e-Print: arXiv:1703.10180

# EXTREME-AXION MATTER



$$\delta'_0 = \left[ -3 \sin \theta - \frac{k^2}{k_J^2} (1 - \cos \theta) \right] \delta_1 + \frac{k^2}{k_J^2} \sin \theta \delta_0 - \frac{\bar{h}'}{2} (1 - \cos \theta),$$

$$\delta'_1 = \left[ -3 \cos \theta - \frac{k^2}{k_J^2} \sin \theta + \frac{\lambda \Omega_\phi}{2y_1} \sin \theta \right] \delta_1 + \left( \frac{k^2}{k_J^2} - \frac{\lambda \Omega_\phi}{2y_1} \right) (1 + \cos \theta) \delta_0 - \frac{\bar{h}'}{2} \sin \theta,$$

$$\lambda = 3 / (8\pi G f^2)$$

Tachyonic effect

Linares, Gonzalez-Morales, U-L, PRD96 (2017) no.6, 061301, e-Print: arXiv:1703.10180

# Viewpoint: The Relentless Hunt for Dark Matter

Dan Hooper

The latest results from two dark matter searches have further ruled out many theoretically attractive dark matter particle candidates.

“Because of the progress of experiments such as XENON1T and PandaX-II, the field of dark matter research is currently in a state of major disruption. The dark matter, it turns out, is not what many of us in the particle theory community imagined it was likely to be.”

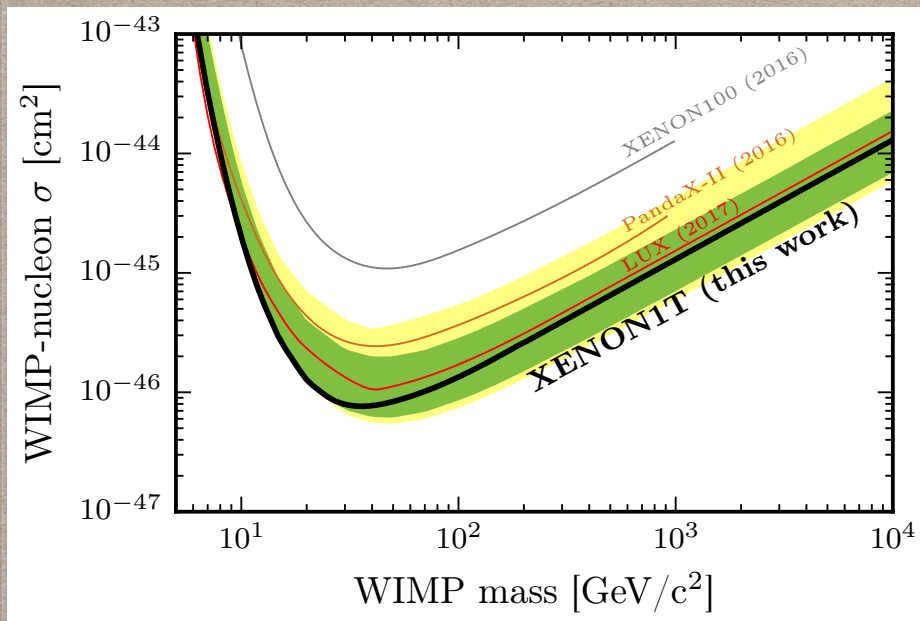
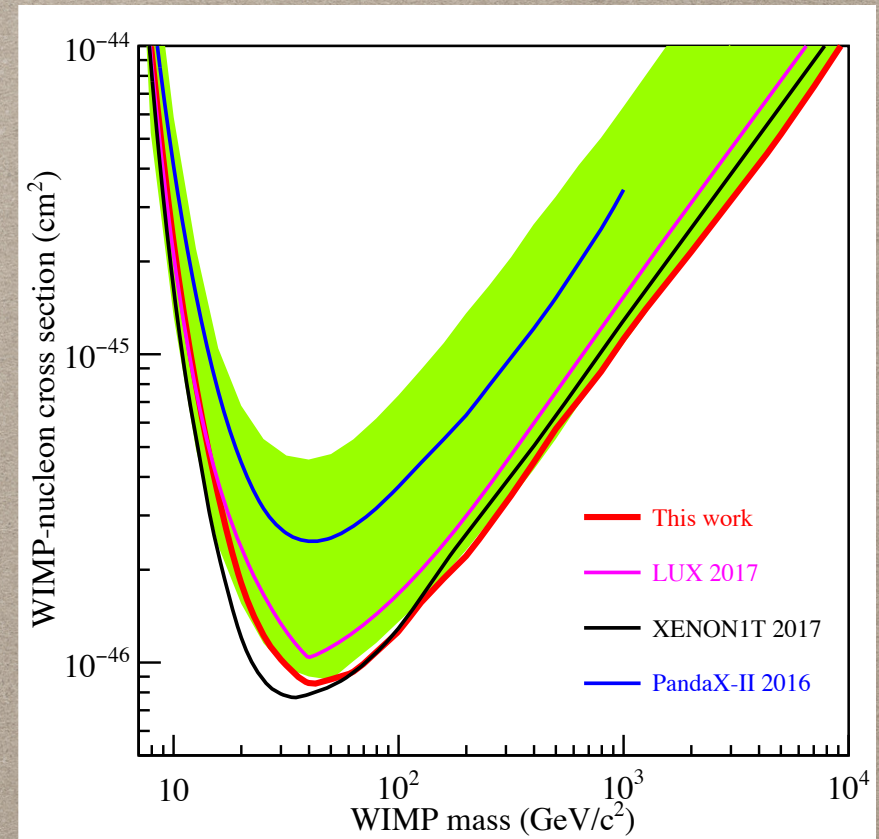


FIG. 4: The spin-independent WIMP-nucleon cross section limits as a function of WIMP mass at 90% confidence level (black) for this run of XENON1T. In green and yellow are the 1- and 2 $\sigma$  sensitivity bands. Results from LUX [27] (red), PandaX-II [28] (brown), and XENON100 [23] (gray) are shown for reference.



(a) log scale in  $m_\chi$

Dark Matter Results From 54-Ton-Day Exposure of PandaX-II Experiment, Phys.Rev.Lett. 119 (2017) no.18, 181302

First Dark Matter Search Results from the XENON1T Experiment, Phys.Rev.Lett. 119 (2017) no.18, 181301

# CONCLUSIONS

- **Scalar fields** are inhabitants of many theories that go **beyond** the Standard Model of Particle Physics
- The existence of scalar fields can imprint **particular signatures** in different cosmological observations (**axiverse**)
- A free **scalar field behaves as dark matter** at large scales, and cosmological observations are able to constraint its mass,  **$m > 10^{-23}$  eV**.
- **Nonlinear formation of structure** seems to prefer lighter bosons, which seems to be **at variance with cosmological observations:  $m < 10^{-22}$  eV**.
- Conflicts are resolved if  **$m = 10^{-21}$  eV**, but this may imply the existence of an **universal soliton profile in the center of all galaxies**.
- More studies of **small scale structure** are required to test further the existence of an **ultra-light boson as the dark matter particle**.